Health benefits attributed to 17α-estradiol, a lifespan-extending compound, are mediated through estrogen receptor α

Shivani N. Mann[1,2,3], Niran Hadad[4], Molly Nelson-Holte[5], Alicia R. Rothman[1], Roshini Sathiaseelan[1], Samim Ali-Mondal[1], Martin-Paul Agbaga[3,6,7], Archana Unnikrishnan[3,8], Malayannan Subramaniam[5], John Hawse[5], Derek M. Huffman[9], Willard M. Freeman[2,10,11], Michael B. Stout[1,2,3]

Institutions:
[1]Department of Nutritional Sciences, University of Oklahoma Health Sciences Center, Oklahoma City, OK
[2]Oklahoma Center for Geroscience, University of Oklahoma Health Sciences Center, Oklahoma City, OK
[3]Harold Hamm Diabetes Center, University of Oklahoma Health Sciences Center, Oklahoma City, OK
[4]The Jackson Laboratory, Bar Harbor, ME
[5]Department of Biochemistry and Molecular Biology, Mayo Clinic, Rochester, MN
[6]Department of Cell Biology, University of Oklahoma Health Sciences Center, Oklahoma City, OK
[7]Dean McGee Eye Institute, University of Oklahoma Health Sciences Center, Oklahoma City, OK
[8]Department of Biochemistry and Molecular Biology, University of Oklahoma Health Sciences Center, Oklahoma City, OK
[9]Department of Molecular Pharmacology, Albert Einstein College of Medicine, New York, NY
[10]Genes & Human Disease Research Program, Oklahoma Medical Research Foundation, Oklahoma City, OK
[11]Oklahoma City Veterans Affairs Medical Center, Oklahoma City, OK

Correspondence To:
Michael B. Stout
1200 N Stonewall Ave, Suite 3057
University of Oklahoma Health Sciences Center
Oklahoma City, OK 73117
Phone: 405-271-2113
Fax: 405-271-1560
michael-stout@ouhsc.edu

Email Addresses of Authors:

Shivani N. Mann	shivani-mann@ouhsc.edu
Niran Hadad	Niran.Hadad@jax.org
Molly Nelson-Holte	NelsonHolte.Molly@mayo.edu
Alicia R. Rothman	Alicia-rothman@ouhsc.edu
Roshini Sathiaseelan	Roshini-sathiaseelan@ouhsc.edu
Samim Ali-Mondal	Samim-alimondal@ouhsc.edu
Martin-Paul Agbaga	martin-paul-agbaga@ouhsc.edu
Archana Unnikrishnan	Archana-Unnikrishnan@ouhsc.edu
Subramaniam Malayannan	Subramaniam.Malayannan@mayo.edu
John Hawse	Hawse.John@mayo.edu
Derek M. Huffman	derek.huffman@einstein.yu.edu
Willard M. Freeman	bill-freeman@omrf.org

ABSTRACT

Aging is the greatest risk factor for most chronic diseases. Metabolic dysfunction underlies several chronic diseases, which are further exacerbated by obesity. Dietary interventions can reverse metabolic declines and slow aging processes, although compliance issues remain paramount due to adverse effects on quality of life. 17α-estradiol treatment improves metabolic parameters and slows aging in male mice. The mechanism by which 17α-E2 elicits benefits remain unknown, which has led speculation that an uncharacterized receptor is involved. Herein, we show that 17α-estradiol and 17β-estradiol elicit similar genomic binding and transcriptional activation of ERα and that the ablation of ERα in male mice completely attenuates the beneficial effects of 17α-estradiol. Our findings also suggest that 17α-E2 acts primarily through the liver and/or hypothalamus to elicit benefits, and that 17α-E2 also improves metabolic parameters in male rats. Collectively, these data suggest ERα is a relevant drug target for mitigating chronic diseases in male mammals.

KEYWORDS

17α-estradiol, aging, estrogen receptor, hypothalamus, liver, metabolism, obesity

INTRODUCTION

Aging is the leading risk factor for most chronic diseases, many of which are associated with declines in metabolic homeostasis [1]. Metabolic detriments associated with advancing age are further exacerbated by obesity [2, 3], which has risen substantially in the older population (> 65 years) over the past several decades [4, 5]. Moreover, obesity in mid-life has been shown to accelerate aging mechanisms and induce phenotypes more commonly observed in older mammals [6-12]. These observations have led many to postulate that obesity may represent a mild progeria syndrome [13-17]. Although it is well established that dietary interventions, including calorie restriction, can reverse obesity-related metabolic sequelae, many of these strategies are not well tolerated in older patients due to concomitant comorbidities [2, 18]. Compliance issues across all age groups also remain a paramount hurdle due to calorie restriction adversely affecting mood, thermoregulation, and musculoskeletal mass [19]. These adverse health outcomes demonstrate the need for pharmacological approaches aimed at curtailing metabolic perturbations associated with obesity and aging.

17α-estradiol (17α-E2) is one of the more recently studied compounds to demonstrate efficacy for beneficially modulating obesity- and age-related health outcomes. The NIA Interventions Testing Program (ITP) found that long-term administration of 17α-E2 extends median lifespan of male mice in a dose-dependent manner [20, 21]. Our group has been exploring potential mechanisms by which 17α-E2 may improve healthspan and extend lifespan in a sex-specific manner. We have found that 17α-E2 administration reduces food intake and regional adiposity in combination with significant improvements in a multitude of systemic metabolic parameters in both middle-aged obese and old male mice without inducing deleterious effects [22-24]. Other groups have also determined that lifelong administration of 17α-E2 beneficially modulates metabolic outcomes, including glucose tolerance, mTORC2 signaling, and hepatic amino acid composition and markers of urea cycling, which were reported to be dependent upon the presence of endogenous androgens [25, 26]. Additionally, multiple lifespan extending compounds, including 17α-E2, exhibit similar modifications in liver function [27]. In all, recent studies by several independent laboratories strongly indicate that the lifespan-extending effects of 17α-E2 are at least associated with, if not dependent on, metabolic improvements.

Despite the mounting evidence demonstrating that 17α-E2 improves numerous health parameters, the signaling mechanism(s) and primary tissues through which 17α-E2 elicits these benefits remain unknown. Although 17α-E2 is a naturally-occurring enantiomer to 17β-estradiol (17β-E2), it has been postulated that 17α-E2 signals through a novel uncharacterized receptor [28-31] as opposed to classical estrogen receptors alpha (ERα) and beta (ERβ); which is due to 17α-E2 having significantly reduced binding affinity to ERα and ERβ as compared to 17β-E2 [32-35]. For this reason, 17α-E2 is often referred to as a non-feminizing estrogen [31, 36, 37]. A few studies have suggested that a novel estrogen receptor, termed ER-X, may mediate 17α-E2 actions in the brain [28-31], although more recent studies supporting this hypothesis are lacking in the literature. Similarly, no reports to date have directly tested whether the doses of 17α-E2 shown to improve healthspan and lifespan in mice are mediated through ERα and/or ERβ.

There is a multitude of data in the diabetes and metabolism literature demonstrating that ERα plays a major role in regulating systemic metabolic parameters. Although most of these studies have historically been performed in female mammals, more recent studies have demonstrated that ERα also plays a critical role in modulating metabolism in male mammals. For instance, Allard and colleagues recently demonstrated that genomic actions of ERα regulate systemic glucose homeostasis in mice of both sexes and insulin production and release in males [38]. Other studies have also determined that hepatic steatosis and insulin sensitivity, and therefore the control of gluconeogenesis, are regulated through FOXO1 in an ERα-dependent manner in male mice [39]. Furthermore, liver-specific deletion of ERα was sufficient to abrogate similar estrogen-mediated metabolic benefits [40, 41]. Given that several reports have linked the administration of 17α-E2 to improvements in metabolic homeostasis, we hypothesized that 17α-E2 signals through ERα to modulate hepatic function and systemic metabolism, thereby contributing to the lifespan-extending effects of 17α-E2.

The work outlined in this report sought to determine if ERα is the signaling mechanism by which 17α-E2 modulates health parameters. As described above, ERα plays a major role in optimizing hepatic function and systemic metabolism, both of which are improved with 17α-E2 treatment. However, no studies to date have tested this potential connection *in vivo.* In this study, we treated obese wild type (WT) and ERα global knockout (ERα KO) littermate mice with 17α-E2 to determine if the ablation of ERα could attenuate 17α-E2-induced benefits on adiposity, metabolic homeostasis, and hepatic function. We observed that the ablation of ERα completely attenuated all beneficial metabolic effects of 17α-E2 in male mice, whereas both WT and ERα KO female mice demonstrated minimal effects on metabolic parameters regardless of genotype. Follow-up studies in male rats undergoing hyperinsulinemic-euglycemic clamps revealed that 17α-E2 acutely modulates hepatic insulin sensitivity through what appears to be direct actions in the liver and/or hypothalamus. These findings strongly suggest that 17α-E2 actions are mediated through ERα and that signaling in the liver and/or hypothalamus may underlie the lifespan-extending effects of 17α-E2 in male mice.

RESULTS

17α-E2 and 17β-E2 similarly modulate transcriptional activity of ERα

It is well established that ligand-mediated ERα dimerization leads to nuclear translocation and transcriptional activity. Previous work has shown that 17α-E2 and 17β-E2 can bind to ERα with different affinities [32-35], yet potential differences in downstream transcriptional activity between the two ligands remains unexplored. To determine if 17α-E2 and 17β-E2 induce similar transcriptional activity of ERα, we assessed ERα DNA binding and transcriptional induction following exposure to 17β-E2 (10nM) or 17α-E2 (10nM or 100nM) in U2OS cells that stably express ERα. We found that 17α-E2 and 17β-E2 induced nearly identical DNA binding signatures and subsequent transcriptional patterns at the doses tested. ChIP sequencing determined that regardless of 17α-E2 or 17β-E2 exposure, the localization of ERα binding to chromatin was nearly identical (Figure 1A). As expected, sequence motifs enriched for ERα binding included WRKY18, hormone response elements (HRE), steroidogenic factor-1 (SF-1), retinoid acid receptor:retinoid X

receptor (RAR:RXR) response elements, nuclear receptor subfamily 5 group A member 2 (Nr5a2), estrogen-related receptor beta (ERRβ), estrogen-related receptor alpha (ERRα), estrogen response elements (ERE), nuclear receptor subfamily 2 group F member 2 (NR2F2), and androgen response elements (ARE) (Figure 1B). Similarly, there were no differences in binding motifs between treatment groups (Figure 1B). Principle component analysis based on whole-transcriptome data revealed that all samples exposed to either 17α-E2 or 17β-E2 clustered together, whereas vehicle treated cells remained distinctly separated (Figure 1C). Heatmap analysis for differentially-expressed genes revealed that both 17α-E2 and 17β-E2 treated samples displayed nearly identical gene suppression and activation signatures as evidenced by the fact that no transcripts were found to be differentially regulated between the estrogen exposures (fdr < 0.05), yet had a strong divergence from vehicle treated cells was seen (Figure 1D, left). Additionally, both 17α-E2 or 17β-E2 treatment conditions resulted in higher ERα DNA binding affinity to gene bodies of these differentially expressed transcripts compared to vehicle treatment, and no differences were observed between 17α-E2 and 17β-E2 conditions (Figure 1D, right). These findings led us to postulate that ERα may be the signaling mechanism by which 17α-E2 modulates health parameters in mice. As such, we subsequently sought to determine if the ablation of ERα *in vivo* would mitigate the effects of 17α-E2.

ERα ablation attenuates 17α-E2-mediated benefits on metabolic parameters *in vivo*

To induce obesity and metabolic perturbations, we fed the mice a high-fat diet for several months prior to initiating 17α-E2 treatment. Almost immediately after 17α-E2 treatment began, WT mice displayed significant reductions in mass (Figure 2A-B) and adiposity (Figure 2C-D). This is aligned with our previous reports demonstrating that 17α-E2 administration quickly reduced body mass and adiposity [22-24], which we have linked to hypothalamic regulation of anorexigenic signaling pathways [23]. Indeed, WT mice in the current study also displayed robust declines in calorie consumption during the first four weeks of treatment (Figure 2E). Conversely, all of these benefits were completely abolished in mice lacking ERα (ERα KO), thereby confirming that 17α-E2 definitively acts through ERα to modulate feeding behaviors, mass, and adiposity. Given the close association between adiposity and metabolic homeostasis, coupled with our previous work demonstrating the ability of 17α-E2 to improve metabolic parameters [22, 23], we also assessed several metabolic variables in these studies. Similar to the mass and adiposity data described above, WT mice receiving 17α-E2 displayed significant improvements in fasting insulin (Figure 3B), HbA1C (Figure 3C), and glucose tolerance (Figure 3D-E & Supplementary Figure 1); whereas ERα KO mice receiving 17α-E2 failed to recapitulate these findings. Interestingly, despite the masses of the WT 17α-E2 treatment group being nearly 15 grams greater than those of the WT chow-fed controls, glucose tolerance was essentially identical between these groups thereby indicating that 17α-E2 restores metabolic flexibility in the presence of obesity (Figure 3D-E & Supplementary Figure 1). We also performed similar analyses in female WT and ERα KO mice and determined that 17α-E2 failed to elicit improvements in mass, adiposity, calorie consumption, or metabolic parameters in either genotype (Supplementary Figure 2). This further supports previous data suggesting 17α-

E2 improves health parameters in a sexually divergent manner [25, 26]. Several studies have implicated ERα in the regulation of systemic metabolic parameters [42]. In particular, liver ERα has been shown to play a critical role in glucose homeostasis, insulin sensitivity, and communication with hypothalamic neurons that modulate metabolism and feeding behavior [43]. This led us to speculate that the liver may play a central role in modulating 17α-E2-mediated effects on systemic metabolic homeostasis.

17α-E2 improves liver disease pathology in an ERα-dependent manner

We previously reported that 17α-E2 alters hepatic lipid deposition and DNA damage responses through unknown mechanisms [22]. In the current study we sought to determine if these findings are mediated through ERα. We found that 17α-E2 significantly reduced liver mass and steatosis as evidenced by reductions in oil-red-O positivity, fatty acid content, and triglyceride accumulation (Figure 4 & Supplementary Figure 3A). These observations were accompanied by significant alterations in gene expression associated with *de novo* lipogenesis (fatty acid synthase [FASN]) and β-oxidation (peroxisome proliferator-activated receptor alpha [PPARα]; sterol regulatory element binding transcription factor 1 [SREBF1]) (Supplementary Figure 3B). These findings are aligned with previous reports showing that 17β-E2 acts through ERα to modulate the expression and activity of genes that regulate hepatic lipid metabolism [44-46]. Interestingly, despite seeing overall reductions in hepatic fatty acid content with 17α-E2 treatment in WT mice (Figure 4C), we also observed elevations in specific fatty acids in these mice as compared to WT HFD controls. Notably, arachidonic acid (AA, 20:4n6) and docosahexaenoic acid (DHA, 22:6n3), both of which are precursors for eicosanoid, resolvin, and protectin production [47, 48], were found to be increased by 17α-E2 treatment in WT mice (Supplementary Figure 4). Our findings are aligned with a previous report by Garratt et al. showing that 17α-E2 increases AA and DHA in liver [26]. None of the 17α-E2-mediated changes in fatty acid profiles were observed in ERα KO mice receiving 17α-E2. In response to the elevations in AA and DHA with 17α-E2 treatment, we also assessed circulating eicosanoids. We found that 17α-E2 treatment also mildly altered several circulating eicosanoid concentrations (Supplementary Table 1). Many of these have been linked to changes in inflammatory signaling [49, 50], although the role they are playing in downstream effects of 17α-E2 on metabolism and/or aging remain unclear.

Due to the association between obesity-related hepatic steatosis and the onset of fibrosis, we assessed collagen deposition by trichrome staining and found that 17α-E2 reduced this in male WT, but not ERα KO, mice (Figure 5A). We also assessed several transcriptional markers of fibrosis and cellular senescence due to a recent report suggesting a link between hepatic fibrosis and senescence in the liver [51]. We found a consistent suppression of fibrosis- and senescence-related gene expression by 17α-E2 in WT mice as evidenced by declines in collagen type 1 alpha 1 (COL1a1), serpin family H member 1 (SERPINH1), cyclin-dependent kinase inhibitor 1 (P21), plasminogen activator inhibitor 1 (PAI1), matrix metallopeptidase 1 (MMP1), matrix metallopeptidase 12 (MMP12), stanniocalcin-1 (STC1), monocyte chemoattractant protein 1 (MCP1), C-X-C motif chemokine ligand 1 (CXCL1), growth differentiation factor 15 (GDF15), and TNF receptor

superfamily member 1A (TNFRSF1A) (Figure 5B). Transcripts predicative of hepatic insulin resistance (1-acylglycerol-3-phosphate O-acyltransferase 5 [AGPAT5], follistatin [FST], inhibin subunit beta E [INHBE], insulin receptor substrate 2 [IRS2]) [52, 53] and gluconeogenesis (glucose 6 phosphatase [G6PC], phosphoenolpyruvate carboxykinase 1 [PCK1], pyruvate kinase [PKM]) [54] also were beneficially modulated by 17α-E2 in WT mice (Supplementary Figure 3C-D). To confirm the ability of 17α-E2 to modulate hepatic insulin sensitivity, we also assessed acute insulin signaling pathways in WT and ERα KO mice (Figure 5C). We found dramatic improvements in phosphorylated AKT (pS473) and FOXO1 (pS256) in WT mice treated with 17α-E2 (Figure 5D-E), whereas these benefits were not observed in ERα KO mice. Our findings are aligned with previous reports demonstrating that hepatic ERα plays a critical role in regulating insulin sensitivity in the liver. Specifically, hepatic ERα is a critical regulator of insulin-induced phosphorylation of AKT and FOXO1 [55]. Collectively, these findings suggest that the liver is highly responsive to 17α-E2 and that a vast majority of these effects are mediated through ERα, including steatosis, fibrosis, senescence, and insulin sensitivity.

Despite our findings consistently demonstrating that 17α-E2 reduces calorie intake and improves liver disease parameters in mice in an ERα dependent manner, it remains unclear if the systemic effects on metabolism are entirely due to long-term reductions in calorie intake. Moreover, it remains unclear if 17α-E2 acts preferentially in a tissue-specific manner and if these observations would also occur in other mammalian species. To address these questions, we next sought to explore the metabolic benefits of 17α-E2 following acute administration in rats.

Acute 17α-E2 administration improves hepatic insulin sensitivity in rats

Our first set of experiments in rats sought to determine if acute peripheral infusions of 17a-E2 modulated metabolic parameters during a hyperinsulinemic-euglycemic clamp (Figure 6A). We found that acute administration of 17α-E2 into the periphery significantly increased glucose infusion rates (GIRs) as compared to vehicle controls (Figure 6B), which was almost entirely due to a suppression of hepatic gluconeogenesis (R_a) (Figure 6C-D). Further supporting direct actions in the liver was our observation of nearly identical glucose disposal rates (R_d) between groups under clamped conditions (Figure 6E). This definitively demonstrates that 17α-E2 can acutely improve metabolic parameters independent of reductions in food intake, and that this appears to be at least partially mediated through actions in the liver. Given that hepatic gluconeogenesis can be modulated both in the liver and through the hypothalamus [56], we sought to evaluate metabolic parameters following the acute administration of 17α-E2 via intracerebroventricular (ICV) infusions into the brain (Figure 6F). To our surprise, we found that central administration of 17α-E2 essentially phenocopied the effects of peripheral 17α-E2 infusion on GIR and hepatic gluconeogenesis (Figure 6G-I). These findings suggest that the two major organ systems responsible for modulating metabolic homeostasis following 17α-E2 treatment are likely the liver and hypothalamus, which we postulate play critical roles in determining the lifespan-extending effects of 17α-E2.

DISCUSSION

17α-E2 has recently been found to increase median lifespan in male mice through uncharacterized mechanisms [20, 21]. We and others have shown that metabolic improvements by 17α-E2 may underlie the lifespan extending effects. In these studies, we sought to determine the role of ERα in 17a-E2 mediated transcriptional effects *in vitro and* metabolic effects *in vivo.* Although previous studies have shown that 17α-E2 has limited binding affinity for ERα, it remains unclear if 17α-E2 can induce transcriptional and physiological alterations in this manner. Given the close association between metabolic improvements and ERα activity, we hypothesized that 17α-E2 signals through ERα to elicit beneficial health outcomes. In these studies, we utilized U2OS cells stably expressing ERα and ERα global knockout mice to assess the involvement of this receptor in mediating 17α-E2 effects. Results from these studies demonstrated that ERα plays a pivotal role in 17α-E2-mediated effects on genomic activity and metabolism, which we surmise underlies the lifespan-extending effects of the compound. Moreover, these data strongly indicate that ERα may play a critical role in determining male lifespan, which in turn suggests that ERα may be a target for the treatment of aging and chronic diseases in males.

Given the similarities between the metabolic benefits observed *in vivo* with 17α-E2 treatment and the established body of literature linking ERα activity to systemic metabolic regulation [42], we used an *in vitro* model to assess specific genomic binding loci and transcriptional activation of ERα by 17α-E2 and 17β-E2. We found that, regardless of dose, 17α-E2 and 17β-E2 elicited nearly identical genomic binding patterns and transcriptional induction. This provides strong evidence that 17α-E2 is likely signaling through ERα to elicit beneficial outcomes, which is contrary to what other reports have suggested [21, 25, 26, 29, 30, 57]. Toran-Allerand et al. reported that 17α-E2 signals through a novel receptor in the brain, which they termed ER-X [29, 57]. Although our findings appear to dispute this notion, several reports have shown that ERα exists and functions as multiple alternatively-spliced variants [58-62]. Therefore, we speculate that ER-X may have been a truncated, alternatively-spliced, form of ERα. These findings led us to investigate how ERα may modulate 17α-E2-induced benefits *in vivo* using ERα global KO mice.

In alignment with our previous reports [22, 23], 17α-E2 reduced food intake, body mass, adiposity, and obesity-related metabolic perturbations in middle-aged WT male mice. Conversely, 17α-E2 failed to elicit these beneficial effects in ERα KO mice, further supporting our hypothesis that ERα is the receptor by which 17α-E2 signals to induce beneficial metabolic outcomes. These observations are similar to how ERα is known to mediate the actions of endogenous estrogens on metabolic parameters in females [42]. In particular, 17β-E2 acts through ERα to regulate systemic insulin sensitivity, lipid distribution, thermogenesis, and hypothalamic anorexigenic pathways [42, 63, 64]. The loss of endogenous estrogen action due to menopause in humans or ovariectomy (OVX) in rodents eliminates these beneficial effects and causes metabolic perturbations and increased visceral adiposity [65]. Moreover, OVX has also been shown to reduce lifespan in female mice [66],

indicating that endogenous estrogens regulate lifespan in females, which we surmise is significantly mediated through ERα. In the current study, 17α-E2 failed to induce beneficial metabolic effects in female mice in either genotype, which we postulate is due to the higher levels of 17β-E2 in females outcompeting 17α-E2 on classical estrogen receptors in WT mice. As alluded to previously, evidence in the literature indicates the binding affinity of 17β-E2 for ERs is dramatically greater than 17α-E2, which has been confirmed with competitive binding assays [32-35]. In males, very few studies have evaluated the role of ERα in metabolism, although a few recent reports have suggested that ERα plays tissue-specific roles, particularly in the liver, by regulating male metabolic homeostasis [38-41, 55]. These studies, coupled with our current findings, led us to speculate that 17α-E2 may be signaling through ERα in the liver to reverse metabolic disease and potentially extend healthspan and/or lifespan in males.

The liver is a major regulator of systemic metabolic homeostasis. Obesity and advancing age often promote a variety of liver conditions, including steatosis, fibrosis, and insulin resistance; all of which are associated with hallmarks of aging [67], including cellular senescence [51], epigenetic alterations [68], and dysregulated nutrient sensing [1]. We have previously shown that 17α-E2 can reduce hepatic steatosis, insulin resistance, and hepatocyte DNA damage through unknown mechanisms [22]. In the present study, we sought to determine if these findings were mediated through ERα. We found that 17α-E2 dramatically reduced liver mass and lipid content. As expected, these observations were not seen in ERα KO mice; again, supporting the hypothesis that 17α-E2 regulates systemic and tissue-specific metabolic parameters through ERα. Interestingly, our findings suggest that 17α-E2 suppresses *de novo* lipogenesis and increases β-oxidation, predominantly through ERα. This is aligned with previous reports showing that 17β-E2 can modulate hepatic lipid dynamics through both genomic and non-genomic mediated actions [69], leading to altered expression of rate limiting enzymes for *de novo* lipogenesis [46] and β-oxidation [70]. Reports have also shown that 17β-E2 can increase triglyceride export, thereby decreasing hepatic lipid deposition [71], and hepatic ERα is critical for the generation of HDL during proestrus [44]. Although we did not directly assess VLDL, we speculate that 17α-E2 reduces hepatic steatosis by increasing VLDL synthesis and/or triglyceride incorporation into VLDL. Additional studies will be needed to confirm how 17α-E2 alters hepatic lipoprotein dynamics.

Hepatic steatosis promotes liver fibrosis, which exacerbates hepatic insulin resistance [72]. In addition to alterations in lipid dynamics, 17α-E2 also dramatically suppressed transcriptional and histological markers of hepatic collagen deposition in an ERα-dependent manner. This was associated with reductions in common hallmarks of cellular senescence, which were also ERα-dependent. This suggests that estrogens may serve a protective role by attenuating chronic liver diseases often seen in obese and/or aged populations. In fact, male humans are at a higher risk of developing hepatic steatosis and fibrosis as compared to age-matched females [73, 74], suggesting a protective role of estrogen signaling on liver function. Additionally, these observations were associated with improvements in hepatic insulin sensitivity, which were not present in ERα KO mice. For

instance, several transcriptional markers of hepatic insulin resistance were suppressed in WT mice receiving 17α-E2, whereas this was almost entirely absent in ERα KO mice. Subsequent studies employing insulin stimulation also revealed that 17α-E2 robustly increased liver AKT and FOXO1 phosphorylation in WT mice, suggesting a reversal of obesity-related hepatic insulin resistance and control of gluconeogenesis. This demonstrates that 17α-E2 modulates hepatic insulin sensitivity in an ERα-dependent manner. Similarly, 17β-E2 acts through ERα to improve glucoregulation in mice [45, 71] and hormone replacement therapy in post-menopausal women is known to improve glucose regulation [75]. This provides further support that 17α-E2 is eliciting metabolic improvements through ERα. These results also implicate the liver as a potential primary target of 17α-E2, due to the ability of hepatic ERα to modulate systemic metabolism and the prominent beneficial effects on liver pathology with 17α-E2 treatment. Hepatic ERα may be a promising target for therapeutics to alleviate metabolic disease. Additionally, the liver may be a primary site through which 17α-E2 improves health parameters and extends lifespan. Future animal studies utilizing cell-type ablation of ERα in the liver will be needed to unravel these possibilities.

Despite the robust effects of 17α-E2 on liver function, it remained unclear if 17α-E2 directly modulates hepatic insulin sensitivity or if these benefits were a secondary response to prolonged reductions in food intake, adiposity, and lipid redistribution. To test this, we performed hyperinsulinemic-euglycemic clamps in conjunction with acute infusions of 17α-E2 in male rats. We found that peripheral infusions of 17α-E2 improved hepatic insulin sensitivity almost immediately, as evidenced by a greater suppression of gluconeogenesis in rats receiving 17α-E2 as compared to vehicle controls. We also did not observe improvements in glucose disposal, which provides additional evidence that 17α-E2-mediated effects are liver-centric. This observation is supported by recent literature demonstrating limited involvement of ERα in skeletal muscle insulin sensitivity [76]. Of particular importance, these findings indicate that 17α-E2 can act acutely to improve hepatic insulin sensitivity, which we speculate is through direct actions on ERα in the liver. Regardless, these findings definitively show that 17α-E2 can improve insulin sensitivity in the absence of chronic reductions in food intake and adiposity. However, it cannot be ruled out that 17α-E2 may be crossing the blood brain barrier and eliciting improvements in hepatic insulin sensitivity via hypothalamic-mediated mechanisms. Several studies have shown that the hypothalamus can regulate hepatic gluconeogenesis through neuronal-mediated mechanisms. Therefore, our next set of experiments delivered 17α-E2 intraventricularly (adjacent to the hypothalamus) during a hyperinsulinemic-euglycemic clamp. These experiments essentially phenocopied the results of the peripheral 17α-E2 infusions, suggesting that the suppression of gluconeogenesis by 17α-E2 is at least partially mediated by the hypothalamus. We surmise that 17α-E2 is likely signaling in both the hypothalamus and liver, which is aligned with previous reports demonstrating significant crosstalk between the hypothalamus and liver to regulate metabolic homeostasis. It is well documented that the arcuate nucleus (ARC) of the hypothalamus is a critical region for regulation of hepatic gluconeogenesis through autonomic regulation and vagus nerve activity [56, 77-79]. Multiple neuronal populations within the hypothalamus known to be involved in the

regulation of systemic metabolism, including Pomc [80], AgRP/NPY [81], and Kisspeptin neurons [82]. Our previous work showed that 17α-E2-mediated reductions of food intake and adiposity are dependent upon functional Pomc neurons in the hypothalamus [23]. This suggests Pomc neurons play a critical role in the downstream effects of 17α-E2 and may be a direct site of action. However, Pomc neuronal activity can be modulated through inhibitory GABA signaling from AgRP neurons, which serve as a counter-regulatory population to Pomc neurons by controlling orexigenic signaling. Therefore, it is possible that 17α-E2-mediated Pomc neuronal activity is regulated by other hypothalamic neuronal populations, in particular AgRP neurons. Both Pomc [83] and AgRP [84, 85] neurons are known to express ERα and both have been implicated in controlling hepatic gluconeogenesis. In addition to potentially signaling through Pomc and/or AgRP neurons in the ARC, Kisspeptin neurons have also been implicated in the control of appetite, adiposity, and metabolic homeostasis [86, 87] and are also responsive to ERα-mediated signaling [88]. Future studies utilizing neuron-specific ERα knockout models will be essential to unraveling the role of the hypothalamus in 17α-E2-mediated effects on metabolism and potentially healthspan and/or lifespan.

Collectively, our findings demonstrate that 17α-E2 acts through ERα in the liver and/or hypothalamus to modulate health parameters. However, our findings are in contrast to other reports suggesting that 17α-E2 elicits health benefits by modulating androgen metabolism [25, 26]. Garratt et al. reported that responsiveness to 17α-E2 was significantly attenuated in castrated male mice [26], which the authors proposed may indicate 17α-E2 acts as a 5α-reductase inhibitor [89] to prevent the conversion of testosterone into dihydrotestosterone (DHT). 17α-E2 is known to be a mild 5α-reductase inhibitor that is prescribed as a topical treatment for androgenetic alopecia [90]. Moreover, 5α-reductase inhibition could conceivably elicit beneficial metabolic effects by either reducing the concentration of DHT, which could decrease adiposity [91, 92], or by promoting greater aromatization of testosterone to 17β-E2 [93], which has been linked to improvements in metabolic parameters [94]. If true, this would imply that the benefits of 17α-E2 are occurring in an indirect manner. However, at the dose used in our studies we do not see dramatic feminization of the sex hormone profiles in male mice [22], which leads us to speculate that 17a-E2 is acting in a direct manner through ERα rather than indirectly through androgen modulation. Furthermore, studies in male rodents [95, 96] and humans [97] demonstrate that 5α-reductase deficiency or inhibition increases insulin resistance and hepatic steatosis and fibrosis, which are contradictory to our consistent findings following 17α-E2 treatment. Despite these contrasting observations, the studies by Garratt et al. do provide important insights into the interconnected and underappreciated relationship between androgen- and estrogen-signaling pathways and their roles in metabolism and aging. For instance, several recent reports have demonstrated interactions between the androgen receptor (AR) and ERα [98-100], which suggests that modulation of one may affect function of the other. Additional factors to consider when comparing and contrasting our studies from those of Garratt et al. are differences in the length of study, age and obesity status of the mice, and counterregulatory and/or compensatory effects of castration. Notably, it is plausible that 17α-E2 could be inducing metabolic benefits

and lifespan-extending effects through several distinct mechanisms, including direct actions through ERα, suppression of DHT production, and/or aromatization of testosterone. Future studies will be needed to discern the potentially interdependent nature of 17α-E2 actions on ERα and androgen metabolism in metabolic improvement and lifespan-extension.

There are a few notable caveats to our studies. First, we utilized constitutive global ERα KO mice, which have been shown to display varying degrees of compensatory ERβ activity due to the absence of ERα during development [101, 102]. However, if compensatory ERβ expression was playing a role in our study, we would not see a complete attenuation of 17α-E2 mediated effects. As such, the results of our studies clearly indicate that ERα is the primary receptor by which 17α-E2 signals. Another potential concern of the model is that ERα KO mice are known to have elevated endogenous testosterone levels [103], although the studies by Garratt et al. would suggest that higher testosterone levels could potentially render the male mice more responsive to 17α-E2, whereas we observed the opposite. Future studies utilizing inducible Cre models to knockdown ERα post-sexual development may be considered if it is determined that tamoxifen-induced Cre induction and subsequent ERα ablation is consistent throughout multiple organ systems, which has been shown to be inconsistent in other reports [104]. Despite these minor concerns related to the model, the use of the constitutive global ERα KO was undoubtedly the best option for our mechanistic studies. Secondly, female ERα KO mice present a greater phenotypic response to the ablation of ERα, leading to obesity and metabolic perturbations early in life, which make them poor comparators to their male counterparts. Despite this, 17α-E2 still failed to elicit beneficial responses in female mice of either genotype (WT or ERα KO) which is aligned with previous reports [25, 26]. Lastly, the current study was relatively short in duration (14 weeks) and it remains unclear if metabolic improvements with 17α-E2 treatment are required for the lifespan extension effects of the compound. Several other studies [20, 21, 25, 26] administered long term treatment of 17α-E2; however, since we were primarily interested in 17α-E2 action from a mechanistic standpoint, a shorter treatment duration was effective in testing our hypothesis. Similarly, given the close relationship between metabolic homeostasis, sex hormones, and longevity [1, 42], we speculate that our short-term observations demonstrate a likely involvement of ERα in male lifespan extension with 17α-E2 treatment. While our current study is not direct evidence of this relationship, it provides critical insight into how hepatic and/or hypothalamic ERα may play a role in healthspan and lifespan extension.

In summary, the results presented here are the first to demonstrate that 17α-E2 induces its numerous metabolic benefits in an ERα-dependent manner. Additional studies will be needed to determine if 17α-E2 predominantly signals through genomic and/or non-genomic functions of ERα. Several recent reports demonstrated that genomic and non-genomic actions of ERα differentially regulate metabolism in a sex specific manner [38, 69], which could potentially explain why females remain unresponsive to 17α-E2. Our results show that 17α-E2 primarily elicits effects in the liver, which is likely due to both direct actions on ERα in

the liver as well as on hypothalamic populations in the brain that regulate metabolism and liver function. We also found that these effects were mirrored by 17α-E2 in rats, indicating that the 17α-E2-mediated effects on metabolic homeostasis occur in multiple mammalian species. Our studies provide critical insight into the molecular mechanisms by which 17α-E2 elicits metabolic benefits, which were previously unknown and may underlie its lifespan extending effects. Future studies should also be performed to determine if cell-type specific signaling through ERα in the liver and/or hypothalamus underlies the metabolic and lifespan-extending effects of 17α-E2.

METHODS

U2OS Cells: Human U2OS osteosarcoma cells stably expressing flag-tagged ERα (U2OS-ERα) under the control of doxycycline (dox) inducible promoter [105] were cultured in phenol-free αMEM medium supplemented with 10% HyCloneTM charcoal/dextran stripped FBS (GE Healthcare Life Sciences, Pittsburgh, PA), 1% antibiotic/antimycotic, 5mg/L blasticidin S, and 500mg/L zeocin in a humidified 37°C incubator with 5% CO_2. Cells were plated in 12-well plates in the presence of doxycycline to induce ERα expression. The following day, cells were treated for 24 hours with 17β-E2 (10nM) or 17α-E2 (10nM and 100nM) (Steraloids, Newport, RI) in charcoal-stripped FBS-containing media.

ChIP-Sequencing and RNA-Sequencing: U2OS-ERα cells were harvested 24 hours post-treatment and chromatin immunoprecipitation was performed as previously described [106, 107]. Briefly, ERα was immunoprecipitated overnight at 4ºC using 10 µg of Flag antibody (clone M2, Sigma-Aldrich, St. Louis, MO). Complexes bound to the antibody were captured with protein G Dynabeads (Thermo Fisher Scientific, Waltham, MA), extensively washed, and reverse cross-linked at 65 ºC overnight. DNA isolation was performed by phenol/chloroform extraction and was used for ChIP-sequencing library preparation. Libraries were sequenced using paired-end 100 bp reads on the Illumina HiSeq 4000 (GSE151039). Reads were aligned to the human genome (hg19, https://genome.ucsc.edu/cgi-bin/hgGateway) using bowtie2 [108]. Duplicated reads were flagged with Picard-tools (http://broadinstitute.github.io/picard/) prior to peak calling using MACS2 [109] with recommended settings. Peak location, breadth, and summit were determined using MACS2, and average peak coverage was extracted from the aligned de-duplicated BAM file and was normalized to total library sequencing depth. Differential peak calling was achieved using MACS2 'bdgdiff' option. Motif analysis was performed using HOMER with standard settings and all identified motifs are included in Supplementary Table 2. Identical experiments were performed in parallel and used for RNA sequencing following RNA extraction and DNase cleanup. RNA libraries were prepared with Illumina's TrueSeq RNA-seq library prep according to manufacturer protocol. Libraries were sequenced with 150 bp paired-end reads on the Illumina 4000 platform (Illumina, San Diego, CA) (GSE151039). Sequence quality control was performed with fastQC, paired reads were trimmed using trimmomatic, and were aligned to the hg19 genome using STAR [110]. Gene counts were

determined in R using the 'summarizeOverlap' function and were used to determine differential expression between treatment groups using the DESeq2 [111] R package.

Control and Experimental Diets: TestDiet, a division of Purina Mills (Richmond, IN), prepared all the diets for studies performed at the University of Oklahoma Health Sciences Center (OUHSC). High-fat fed male mice received TestDiet 58V8 (35.5% CHO, 18.3% PRO, 45.7% FAT) or TestDiet 58Y1 (20.3% CHO, 18.1% PRO, 61.6% FAT) ± 17α-E2 (14.4 ppm; Steraloids) as detailed below. Chow-fed male and female mice received TestDiet 58YP (66.6% CHO, 20.4% PRO, 13.0% FAT) ± 17α-E2 (14.4 ppm; Steraloids, Newport, RI) as detailed below. Fisher-Brown Norway (FBN) F1 hybrid male rats received Purina 5001 (58.0% CHO, 28.5% PRO, 13.5% FAT) as detailed below.

Animals: Wild-type (WT) and ERα KO littermate mice were acquired from Dr. Kenneth Korach (National Institute of Environmental Health Sciences [NIEHS]) and were also breed at OUHSC by pairing ERα heterozygous KO mice. Mice acquired from Dr. Korach and The Jackson Laboratory (JAX; strain #026176) were generated from identical founder strains in the laboratory of Dr. Korach at NIEHS. Age-matched, WT male, chow-fed (TestDiet 58YP), control mice were purchased from JAX (strain #000664). For experimental interventions all mice were individually housed with ISO cotton pad bedding, cardboard enrichment tubes, and nestlets at 22 ± 0.5°C on a 12:12-hour light-dark cycle. Unless otherwise noted, all mice had ad libitum access to food and water throughout the experimental timeframe. WT FBN-F1 hybrid male rats were obtained from the NIA breeding colony at Charles River. Unless otherwise noted, all rats were individually housed with corncob bedding at 22 ± 0.5°C on a 14:10-hour light-dark cycle with *ad libitum* access to food and water. All animal procedures were reviewed and approved by the Institutional Animal Care and Use Committees at OUHSC and the Einstein College of Medicine.

Animal Study 1: Male ERα WT and KO mice were high-fat fed (HFD; TestDiet 58V8) for 4 months prior to study initiation to induce obesity and metabolic perturbations. Age-matched, WT male, chow-fed, control mice were maintained on TestDiet 58YP throughout the entire study. At the conclusion of the fatting period, all mice (age: 6-8 months) receiving HFD were randomized within genotype by age, body mass, fat mass, calorie intake, fasting glucose, fasting insulin, and glycosylated hemoglobin (HbA1C) into HFD or HFD+17α-E2 (TestDiet 58V8 + 17α-E2) treatment groups for a 14-week intervention. Body mass and food intake were assessed daily for the first 4 weeks, followed by body mass and body composition (EchoMRI, Houston, TX) on a weekly basis. At the conclusion of the study, mice were euthanized with isoflurane in the fasted state (5-6 hours). Blood was collected into EDTA-lined tubes by cardiac puncture, and plasma was collected and frozen. Tissues were excised, weighed, flash frozen, and stored at −80°C unless otherwise noted. Small sections of liver were fixed in 4% paraformaldehyde in preparation for paraffin- or cryo-embedding for future analyses.

Animal Study 2: Female WT and ERα KO mice were maintained on TestDiet 58YP until animal study 1 was ready to begin so the two studies could be performed in parallel. At this time, all mice (age: 9-11 months) were randomized within genotype by age, body mass, fat mass, calorie intake, fasting glucose, fasting insulin, and glycosylated hemoglobin (HbA1C) into chow or chow+17α-E2 (TestDiet 58YP + 17α-E2) treatment groups. The study was terminated following a 4-week intervention due to a lack of responsiveness to 17α-E2. Physiological parameters and animal dissections were performed as described in animal study 1.

Animal Study 3: Male ERα WT and KO mice were high-fat fed (HFD; TestDiet 58Y1) for 4 months prior to study initiation to induce obesity and metabolic perturbations. As was done in animal study 1, age-matched, WT male, chow-fed, control mice were maintained on TestDiet 58YP throughout the entire study. At the conclusion of the fatting period, all mice (age: 6 months) receiving HFD were randomized within genotype by body mass, fat mass, calorie intake, fasting glucose, and fasting insulin into HFD or HFD+17α-E2 (TestDiet 58Y1 + 17α-E2) treatment groups for a 12-week intervention. Prior to being euthanized, mice were fasted (5-6 hours) and IP injected with insulin (Novolin R® 100 U/ml; 2mU/g) to assess tissue-specific insulin sensitivity as previously described [112]. Each mouse was euthanized 15 minutes following their insulin injection and dissection procedures were performed as outlined in animal study 1.

Animal Study 4: FBN-F1 hybrid male rats were acclimated to the animal facilities within the Einstein Nathan Shock Center for two weeks prior to undergoing surgeries in preparation for hyperinsulinemic-euglycemic clamp studies. All surgeries were conducted under 2% isoflurane. For clamp studies incorporating central infusions, rats underwent two surgical procedures. First, stereotactic placement of a steel-guide cannula (Plastics One, Roanoke, VA) reaching the 3rd ventricle was performed. The implant was secured in place with dental cement and animals were treated with analgesic as needed. Approximately 14 days later, animals underwent a second surgical procedure to place indwelling catheters into the right internal jugular vein and the left carotid artery, which was also performed for animals undergoing only peripheral clamp studies. Hyperinsulinemic-euglycemic clamp studies incorporating peripheral 17α-E2 infusions were performed as previously described [113]. For studies employing peripheral infusions of 17α-E2, 17α-E2 was diluted in sterile saline to a final concentration of 30ng/ul. Beginning at t=0min animals received a primed-continuous infusion of saline or 30ng/ul 17α-E2 provided as a 3ug bolus at a rate of 20ul/min over 5min, followed by a continuous infusion at a rate of 0.06ml/hr over 235min (9.4ng/hr) for a maintenance dose of 7ug (total dose 10ug). Hyperinsulinemic-euglycemic clamp studies with intracerebroventricular (ICV) infusions were performed as previously described [114]. 17α-E2 powder (Steraloids) was dissolved in DMSO at a concentration of 10mg/ml and stored at -80°C. For ICV infusions, 17α-E2 was diluted in artificial cerebral spinal fluid (ACSF) to a final concentration of 2ng/ul. Beginning at t=0min, animals received a primed-continuous ICV infusion of ACSF (Vehicle) or 17α-E2 (17α) provided as a 15ng bolus at a rate of 1ul/min over 7.5min, followed by a continuous infusion of 56.5ng at a rate of 0.08ul/hr over 6hr (9.4ng/hr) and a total dose of 71.5ng.

In Vivo Metabolic Analyses in Mice: Unless otherwise noted, all experiments requiring fasting conditions were performed in the afternoon, 5-6 hours following the removal of food as outlined elsewhere [115]. To ensure fasting conditions, mice were transferred to clean cages containing ISO cotton padding and clean cardboard enrichment tubes. Fasting glucose was evaluated using a Bayer Breeze 2 Blood Glucose Monitoring System (Bayer Global, Leverkusen, Germany). Fasting insulin was evaluated using a Mouse Ultrasensitive Insulin ELISA from Alpco (Salem, NH). HbA1c was assessed by A1C-Now Monitoring kits (Bayer, Whippany, NJ). Glucose tolerance tests were performed following a 5-hour fast using an intraperitoneal filtered dextrose injection of 1g/kg body mass [116]. Blood glucose was measured immediately pre-injection (time 0) and at 15, 30, 60, 90, and 120 minutes post injection.

Liver Histology: Liver oil-red-O and Masson's trichrome staining were performed by the Oklahoma Medical Research Foundation Imaging Core Facility using previously reported methodology [117, 118]. Oil-red-O lipid staining was blindly quantified from 10 images per animal using ImageJ.

Liver Triglycerides: Liver samples (~100 mg) were homogenized on ice for 60 seconds in 10X (v/w) Cell Signaling Lysis Buffer (Cell Signaling, Danvers, MA) with protease and phosphatase inhibitors (Boston BioProducts, Boston, MA). Total lipid was extracted using the Folch method [119] and final triglyceride concentrations were determined using a spectrophotometric assay as previously described [120].

Liver Fatty Acids: Liver samples (~50 mg) were homogenized and on ice for 60 seconds in 10X (v/w) Cell Signaling Lysis Buffer (Cell Signaling, Danvers, MA) with protease and phosphatase inhibitors (Boston BioProducts, Boston, MA). Total lipid was extracted using the Folch method [119] and lipid extracts were dried down under nitrogen gas. Total lipid was then converted to fatty acid methyl esters and were identified by GC-MS and GC-FID as previously described [121, 122].

Plasma Eicosanoids: Plasma eicosanoid analyses were performed by the UCSD Lipidomics Core as described previously [123].

Real-time PCR: Total RNA was extracted using Trizol (Life Technologies, Carlsbad, CA) and was reverse transcribed to cDNA with the High-Capacity cDNA Reverse Transcription kit (Applied Biosystems, Foster City, CA). Real-time PCR was performed in a QuantStudio 12K Flex Real Time PCR System (Thermofisher Scientific, Waltham, MA) using TaqMan™ Gene Expression Master Mix (Applied Biosystems/Thermofisher Scientific, Waltham, MA) and predesigned gene expression assays with FAM probes from Integrated DNA Technologies (Skokie, Illinois). Target gene expression was expressed as $2^{-\Delta\Delta CT}$ by the comparative CT method [124] and normalized to the expression of TATA-Box Binding Protein (TBP) in liver.

Western Blotting: Liver was homogenized in RIPA Buffer (Cell Signaling, Danvers, MA) with protease and phosphatase inhibitors (Boston Bioproducts, Boston, MA). Total protein was quantified using BCA Protein Assay Reagent Kit (Pierce, Rockford, IL). Proteins were separated on an Any kD™ Criterion™ TGX Stain-Free™ Protein Gel (Biorad, Hercules, CA) and transferred to nitrocellulose membranes, 0.2 µm pore size (Biorad, Hercules, CA). Primary antibodies used were α-pS256 FOX01 (Abcam ab131339, 1:1000), α-FOX01a (Abcam ab52857, 1:1000), α-pS473 AKT (Abcam ab81283, 1:3000), α-pan-AKT (Abcam ab179463, 1:10000), α-GAPDH (Abcam ab9485, 1:2500). Primary antibody detection was performed with IRDye® 800CW Infrared α-Rabbit (LI-COR Biotechnology, Lincoln, NE) at 1:15000 concentration. Blot imaging was done on Odyssey Fc Imaging System (LI-COR Biotechnology, Lincoln, NE) and protein detection and quantification was performed with Image Studio Software (LI-COR Biotechnology, Lincoln, NE).

Statistical Analyses: Analyses of differences between groups were performed by 2-way ANOVA, 2-way repeated measures ANOVA, or Student's t-test where appropriate using SigmaPlot 12.5 Software. Values are presented as mean ± SEM with *p* values less than 0.05 considered to be significant unless otherwise specified.

ACKNOWLEDGEMENTS

We thank Dr. Kenneth Korach at the National Institute of Environmental Health Sciences for providing ERα KO and WT littermate mice. We also thank Dr. Lora Bailey-Downs, Richard Brush, and Michael Sullivan for technical support. This work was supported by the National Institutes of Health (R00 AG51661 to M.B.S., T32 AG052363 to S.N.M., & R01 EY030513 to M-P.A.) and Pilot Research Funding from the Harold Hamm Diabetes Center (M.B.S. and S.N.M.), Einstein Nathan Shock Center (P30 AG038072) of Excellence in the Basic Biology of Aging (M.B.S.), and OUHSC Lipidomics Core (P30 EY012190).

AUTHOR CONTRIBUTIONS

S.N.M. and M.B.S. conceived the project and designed the experiments. S.N.M., A.R.R., and R.S., performed the experiments with contributions from M.N-H., S.A-M., M-P.A., A.U., M.S., J.H., and D.M.H. N.H. and W.M.F. performed bioinformatic analyses. S.N.M. and M.B.S. wrote the manuscript and all authors edited and approved the final manuscript.

COMPETING INTERESTS

The authors declare no conflicts or competing interests.

REFERENCES

1. Lopez-Otin, C., et al., *The hallmarks of aging.* Cell, 2013. **153**(6): p. 1194-217.
2. Villareal, D.T., et al., *Obesity in older adults: technical review and position statement of the American Society for Nutrition and NAASO, The Obesity Society.* Obesity research, 2005. **13**(11): p. 1849-63.
3. Waters, D.L., A.L. Ward, and D.T. Villareal, *Weight loss in obese adults 65years and older: a review of the controversy.* Exp Gerontol, 2013. **48**(10): p. 1054-61.
4. Flegal, K.M., et al., *Prevalence and trends in obesity among US adults, 1999-2008.* JAMA, 2010. **303**(3): p. 235-41.
5. Flegal, K.M., et al., *Trends in Obesity Among Adults in the United States, 2005 to 2014.* JAMA, 2016. **315**(21): p. 2284-91.
6. Bischof, G.N. and D.C. Park, *Obesity and Aging: Consequences for Cognition, Brain Structure, and Brain Function.* Psychosom Med, 2015. **77**(6): p. 697-709.
7. Horvath, S., et al., *Obesity accelerates epigenetic aging of human liver.* Proceedings of the National Academy of Sciences of the United States of America, 2014. **111**(43): p. 15538-43.
8. Nevalainen, T., et al., *Obesity accelerates epigenetic aging in middle-aged but not in elderly individuals.* Clin Epigenetics, 2017. **9**: p. 20.
9. Yang, H., et al., *Obesity accelerates thymic aging.* Blood, 2009. **114**(18): p. 3803-12.
10. Whitmer, R.A., et al., *Obesity in middle age and future risk of dementia: a 27 year longitudinal population based study.* BMJ, 2005. **330**(7504): p. 1360.
11. Whitmer, R.A., et al., *Midlife cardiovascular risk factors and risk of dementia in late life.* Neurology, 2005. **64**(2): p. 277-81.
12. Dye, L., et al., *The relationship between obesity and cognitive health and decline.* Proc Nutr Soc, 2017. **76**(4): p. 443-454.
13. Salvestrini, V., C. Sell, and A. Lorenzini, *Obesity May Accelerate the Aging Process.* Front Endocrinol (Lausanne), 2019. **10**: p. 266.
14. Tzanetakou, I.P., et al., *"Is obesity linked to aging?": adipose tissue and the role of telomeres.* Ageing research reviews, 2012. **11**(2): p. 220-9.
15. Perez, L.M., et al., *'Adipaging': ageing and obesity share biological hallmarks related to a dysfunctional adipose tissue.* J Physiol, 2016. **594**(12): p. 3187-207.
16. Tchkonia, T., et al., *Fat tissue, aging, and cellular senescence.* Aging cell, 2010. **9**(5): p. 667-84.
17. Stout, M.B., et al., *Physiological Aging: Links Among Adipose Tissue Dysfunction, Diabetes, and Frailty.* Physiology (Bethesda), 2017. **32**(1): p. 9-19.
18. Jensen, M.D., et al., *2013 AHA/ACC/TOS guideline for the management of overweight and obesity in adults: a report of the American College of Cardiology/American Heart Association Task Force on Practice Guidelines and The Obesity Society.* Circulation, 2014. **129**(25 Suppl 2): p. S102-38.
19. Dirks, A.J. and C. Leeuwenburgh, *Caloric restriction in humans: potential pitfalls and health concerns.* Mechanisms of ageing and development, 2006. **127**(1): p. 1-7.
20. Strong, R., et al., *Longer lifespan in male mice treated with a weakly estrogenic agonist, an antioxidant, an alpha-glucosidase inhibitor or a Nrf2-inducer.* Aging Cell, 2016. **15**(5): p. 872-84.
21. Harrison, D.E., et al., *Acarbose, 17-alpha-estradiol, and nordihydroguaiaretic acid extend mouse lifespan preferentially in males.* Aging cell, 2014. **13**(2): p. 273-82.
22. Stout, M.B., et al., *17alpha-Estradiol Alleviates Age-related Metabolic and Inflammatory Dysfunction in Male Mice Without Inducing Feminization.* J Gerontol A Biol Sci Med Sci, 2017. **72**(1): p. 3-15.
23. Steyn, F.J., et al., *17alpha-estradiol acts through hypothalamic pro-opiomelanocortin expressing neurons to reduce feeding behavior.* Aging Cell, 2018. **17**(1).
24. Miller, B.F., et al., *Short-term calorie restriction and 17alpha-estradiol administration elicit divergent effects on proteostatic processes and protein content in metabolically active tissues.* J Gerontol A Biol Sci Med Sci, 2019.
25. Garratt, M., et al., *Sex differences in lifespan extension with acarbose and 17-alpha estradiol: gonadal hormones underlie male-specific improvements in glucose tolerance and mTORC2 signaling.* Aging Cell, 2017. **16**(6): p. 1256-1266.
26. Garratt, M., et al., *Male lifespan extension with 17-alpha estradiol is linked to a sex-specific metabolomic response modulated by gonadal hormones in mice.* Aging Cell, 2018. **17**(4): p. e12786.

27. Tyshkovskiy, A., et al., *Identification and Application of Gene Expression Signatures Associated with Lifespan Extension.* Cell Metab, 2019. **30**(3): p. 573-593 e8.
28. Toran-Allerand, C.D., *Estrogen and the brain: beyond ER-alpha, ER-beta, and 17beta-estradiol.* Annals of the New York Academy of Sciences, 2005. **1052**: p. 136-44.
29. Toran-Allerand, C.D., et al., *ER-X: a novel, plasma membrane-associated, putative estrogen receptor that is regulated during development and after ischemic brain injury.* J Neurosci, 2002. **22**(19): p. 8391-401.
30. Toran-Allerand, C.D., et al., *17alpha-estradiol: a brain-active estrogen?* Endocrinology, 2005. **146**(9): p. 3843-50.
31. Green, P.S. and J.W. Simpkins, *Estrogens and estrogen-like non-feminizing compounds. Their role in the prevention and treatment of Alzheimer's disease.* Annals of the New York Academy of Sciences, 2000. **924**: p. 93-8.
32. Edwards, D.P. and W.L. McGuire, *17 alpha-Estradiol is a biologically active estrogen in human breast cancer cells in tissue culture.* Endocrinology, 1980. **107**(4): p. 884-91.
33. Korenman, S.G., *Comparative binding affinity of estrogens and its relation to estrogenic potency.* Steroids, 1969. **13**(2): p. 163-77.
34. Littlefield, B.A., et al., *A simple and sensitive microtiter plate estrogen bioassay based on stimulation of alkaline phosphatase in Ishikawa cells: estrogenic action of delta 5 adrenal steroids.* Endocrinology, 1990. **127**(6): p. 2757-62.
35. Anstead, G.M., K.E. Carlson, and J.A. Katzenellenbogen, *The estradiol pharmacophore: ligand structure-estrogen receptor binding affinity relationships and a model for the receptor binding site.* Steroids, 1997. **62**(3): p. 268-303.
36. Engler-Chiurazzi, E.B., D.F. Covey, and J.W. Simpkins, *A novel mechanism of non-feminizing estrogens in neuroprotection.* Exp Gerontol, 2016.
37. Kaur, S.P., S. Bansal, and K. Chopra, *17alpha-Estradiol: a candidate neuroserm and non-feminizing estrogen for postmenopausal neuronal complications.* Steroids, 2015. **96**: p. 7-15.
38. Allard, C., et al., *Loss of Nuclear and Membrane Estrogen Receptor-alpha Differentially Impairs Insulin Secretion and Action in Male and Female Mice.* Diabetes, 2019. **68**(3): p. 490-501.
39. Yan, H., et al., *Estrogen Improves Insulin Sensitivity and Suppresses Gluconeogenesis via the Transcription Factor Foxo1.* Diabetes, 2019. **68**(2): p. 291-304.
40. Guillaume, M., et al., *Selective Liver Estrogen Receptor alpha Modulation Prevents Steatosis, Diabetes, and Obesity Through the Anorectic Growth Differentiation Factor 15 Hepatokine in Mice.* Hepatol Commun, 2019. **3**(7): p. 908-924.
41. Qiu, S., et al., *Hepatic estrogen receptor alpha is critical for regulation of gluconeogenesis and lipid metabolism in males.* Sci Rep, 2017. **7**(1): p. 1661.
42. Barros, R.P. and J.A. Gustafsson, *Estrogen receptors and the metabolic network.* Cell Metab, 2011. **14**(3): p. 289-99.
43. Torre, D., et al., *Sexual Dimorphism and Estrogen Action in Mouse Liver.* Adv Exp Med Biol, 2017. **1043**: p. 141-151.
44. Della Torre, S., et al., *An Essential Role for Liver ERalpha in Coupling Hepatic Metabolism to the Reproductive Cycle.* Cell Rep, 2016. **15**(2): p. 360-71.
45. Stubbins, R.E., et al., *Estrogen modulates abdominal adiposity and protects female mice from obesity and impaired glucose tolerance.* Eur J Nutr, 2012. **51**(7): p. 861-70.
46. Zhang, H., et al., *Differential effects of estrogen/androgen on the prevention of nonalcoholic fatty liver disease in the male rat.* J Lipid Res, 2013. **54**(2): p. 345-57.
47. Szefel, J., W.J. Kruszewski, and E. Sobczak, *Factors influencing the eicosanoids synthesis in vivo.* Biomed Res Int, 2015. **2015**: p. 690692.
48. Kohli, P. and B.D. Levy, *Resolvins and protectins: mediating solutions to inflammation.* Br J Pharmacol, 2009. **158**(4): p. 960-71.
49. Kiss, L., et al., *Epoxyeicosatrienoates are the dominant eicosanoids in human lungs upon microbial challenge.* Eur Respir J, 2010. **36**(5): p. 1088-98.
50. Gilroy, D.W., et al., *CYP450-derived oxylipins mediate inflammatory resolution.* Proc Natl Acad Sci U S A, 2016. **113**(23): p. E3240-9.

51. Ogrodnik, M., et al., *Cellular senescence drives age-dependent hepatic steatosis.* Nat Commun, 2017. **8**: p. 15691.
52. Tao, R., et al., *Inactivating hepatic follistatin alleviates hyperglycemia.* Nat Med, 2018. **24**(7): p. 1058-1069.
53. Parks, B.W., et al., *Genetic architecture of insulin resistance in the mouse.* Cell Metab, 2015. **21**(2): p. 334-347.
54. Xiong, Y., et al., *Regulation of glycolysis and gluconeogenesis by acetylation of PKM and PEPCK.* Cold Spring Harb Symp Quant Biol, 2011. **76**: p. 285-9.
55. Zhu, L., et al., *Estrogen signaling prevents diet-induced hepatic insulin resistance in male mice with obesity.* Am J Physiol Endocrinol Metab, 2014. **306**(10): p. E1188-97.
56. Zhang, X., et al., *Unraveling the Regulation of Hepatic Gluconeogenesis.* Front Endocrinol (Lausanne), 2018. **9**: p. 802.
57. Toran-Allerand, C.D., *Estrogen and the brain: beyond ER-alpha, ER-beta, and 17beta-estradiol.* Ann N Y Acad Sci, 2005. **1052**: p. 136-44.
58. Flouriot, G., et al., *Differentially expressed messenger RNA isoforms of the human estrogen receptor-alpha gene are generated by alternative splicing and promoter usage.* Mol Endocrinol, 1998. **12**(12): p. 1939-54.
59. Wang, Z., et al., *Identification, cloning, and expression of human estrogen receptor-alpha36, a novel variant of human estrogen receptor-alpha66.* Biochem Biophys Res Commun, 2005. **336**(4): p. 1023-7.
60. Taylor, S.E., P.L. Martin-Hirsch, and F.L. Martin, *Oestrogen receptor splice variants in the pathogenesis of disease.* Cancer Lett, 2010. **288**(2): p. 133-48.
61. Zhang, J., et al., *Alternative splicing of estrogen receptor alpha in hepatocellular carcinoma.* BMC Cancer, 2016. **16**(1): p. 926.
62. Lin, A.H., et al., *Differential ligand binding affinities of human estrogen receptor-alpha isoforms.* PLoS One, 2013. **8**(4): p. e63199.
63. Stincic, T.L., O.K. Ronnekleiv, and M.J. Kelly, *Diverse actions of estradiol on anorexigenic and orexigenic hypothalamic arcuate neurons.* Horm Behav, 2018. **104**: p. 146-155.
64. Lopez, M. and M. Tena-Sempere, *Estrogens and the control of energy homeostasis: a brain perspective.* Trends Endocrinol Metab, 2015. **26**(8): p. 411-21.
65. Stefanska, A., K. Bergmann, and G. Sypniewska, *Metabolic Syndrome and Menopause: Pathophysiology, Clinical and Diagnostic Significance.* Adv Clin Chem, 2015. **72**: p. 1-75.
66. Benedusi, V., et al., *Ovariectomy shortens the life span of female mice.* Oncotarget, 2015. **6**(13): p. 10801-11.
67. Hunt, N.J., et al., *Hallmarks of Aging in the Liver.* Comput Struct Biotechnol J, 2019. **17**: p. 1151-1161.
68. Horvath, S., et al., *Obesity accelerates epigenetic aging of human liver.* Proc Natl Acad Sci U S A, 2014. **111**(43): p. 15538-43.
69. Pedram, A., et al., *Membrane and nuclear estrogen receptor alpha collaborate to suppress adipogenesis but not triglyceride content.* FASEB J, 2016. **30**(1): p. 230-40.
70. Camporez, J.P., et al., *Cellular mechanism by which estradiol protects female ovariectomized mice from high-fat diet-induced hepatic and muscle insulin resistance.* Endocrinology, 2013. **154**(3): p. 1021-8.
71. Zhu, L., et al., *Estrogen treatment after ovariectomy protects against fatty liver and may improve pathway-selective insulin resistance.* Diabetes, 2013. **62**(2): p. 424-34.
72. Kim, I.H., T. Kisseleva, and D.A. Brenner, *Aging and liver disease.* Curr Opin Gastroenterol, 2015. **31**(3): p. 184-91.
73. Guy, J. and M.G. Peters, *Liver disease in women: the influence of gender on epidemiology, natural history, and patient outcomes.* Gastroenterol Hepatol (N Y), 2013. **9**(10): p. 633-9.
74. Collaborators, G.B.D.C., *The global, regional, and national burden of cirrhosis by cause in 195 countries and territories, 1990-2017: a systematic analysis for the Global Burden of Disease Study 2017.* Lancet Gastroenterol Hepatol, 2020. **5**(3): p. 245-266.
75. Rossi, R., G. Origliani, and M.G. Modena, *Transdermal 17-beta-estradiol and risk of developing type 2 diabetes in a population of healthy, nonobese postmenopausal women.* Diabetes Care, 2004. **27**(3): p. 645-9.

76. Inigo, M.R., et al., *Estrogen receptor-alpha in female skeletal muscle is not required for regulation of muscle insulin sensitivity and mitochondrial regulation.* Mol Metab, 2020. **34**: p. 1-15.
77. Pocai, A., et al., *A brain-liver circuit regulates glucose homeostasis.* Cell Metab, 2005. **1**(1): p. 53-61.
78. Brandt, C., et al., *Food Perception Primes Hepatic ER Homeostasis via Melanocortin-Dependent Control of mTOR Activation.* Cell, 2018. **175**(5): p. 1321-1335 e20.
79. Ruud, J., S.M. Steculorum, and J.C. Bruning, *Neuronal control of peripheral insulin sensitivity and glucose metabolism.* Nat Commun, 2017. **8**: p. 15259.
80. Dodd, G.T., et al., *Insulin regulates POMC neuronal plasticity to control glucose metabolism.* Elife, 2018. **7**.
81. Konner, A.C., et al., *Insulin action in AgRP-expressing neurons is required for suppression of hepatic glucose production.* Cell Metab, 2007. **5**(6): p. 438-49.
82. Nestor, C.C., M.J. Kelly, and O.K. Ronnekleiv, *Cross-talk between reproduction and energy homeostasis: central impact of estrogens, leptin and kisspeptin signaling.* Horm Mol Biol Clin Investig, 2014. **17**(3): p. 109-28.
83. Xu, Y., et al., *Distinct hypothalamic neurons mediate estrogenic effects on energy homeostasis and reproduction.* Cell Metab, 2011. **14**(4): p. 453-65.
84. Sar, M., et al., *Localization of neuropeptide-Y immunoreactivity in estradiol-concentrating cells in the hypothalamus.* Endocrinology, 1990. **127**(6): p. 2752-6.
85. Benedusi, V., et al., *Liver ERalpha regulates AgRP neuronal activity in the arcuate nucleus of female mice.* Sci Rep, 2017. **7**(1): p. 1194.
86. Rao, Y.S., N.N. Mott, and T.R. Pak, *Effects of kisspeptin on parameters of the HPA axis.* Endocrine, 2011. **39**(3): p. 220-8.
87. Wolfe, A. and M.A. Hussain, *The Emerging Role(s) for Kisspeptin in Metabolism in Mammals.* Front Endocrinol (Lausanne), 2018. **9**: p. 184.
88. Dubois, S.L., et al., *Positive, but not negative feedback actions of estradiol in adult female mice require estrogen receptor alpha in kisspeptin neurons.* Endocrinology, 2015. **156**(3): p. 1111-20.
89. Schriefers, H., et al., *[Inhibition of testosterone metabolism by 17-alpha-estradiol in rat liver slices].* Arzneimittelforschung, 1991. **41**(11): p. 1186-9.
90. Orfanos, C.E. and L. Vogels, *[Local therapy of androgenetic alopecia with 17 alpha-estradiol. A controlled, randomized double-blind study (author's transl)].* Dermatologica, 1980. **161**(2): p. 124-32.
91. Moverare-Skrtic, S., et al., *Dihydrotestosterone treatment results in obesity and altered lipid metabolism in orchidectomized mice.* Obesity (Silver Spring), 2006. **14**(4): p. 662-72.
92. Bolduc, C., et al., *Effects of dihydrotestosterone on adipose tissue measured by serial analysis of gene expression.* J Mol Endocrinol, 2004. **33**(2): p. 429-44.
93. Veldhuis, J.D., et al., *Aromatase and 5alpha-reductase inhibition during an exogenous testosterone clamp unveils selective sex steroid modulation of somatostatin and growth hormone secretagogue actions in healthy older men.* J Clin Endocrinol Metab, 2009. **94**(3): p. 973-81.
94. Rubinow, K.B., *Estrogens and Body Weight Regulation in Men.* Adv Exp Med Biol, 2017. **1043**: p. 285-313.
95. Livingstone, D.E., et al., *5alpha-Reductase type 1 deficiency or inhibition predisposes to insulin resistance, hepatic steatosis, and liver fibrosis in rodents.* Diabetes, 2015. **64**(2): p. 447-58.
96. Dowman, J.K., et al., *Loss of 5alpha-reductase type 1 accelerates the development of hepatic steatosis but protects against hepatocellular carcinoma in male mice.* Endocrinology, 2013. **154**(12): p. 4536-47.
97. Wei, L., et al., *Incidence of type 2 diabetes mellitus in men receiving steroid 5alpha-reductase inhibitors: population based cohort study.* BMJ, 2019. **365**: p. l1204.
98. D'Amato, N.C., et al., *Cooperative Dynamics of AR and ER Activity in Breast Cancer.* Mol Cancer Res, 2016. **14**(11): p. 1054-1067.
99. Panet-Raymond, V., et al., *Interactions between androgen and estrogen receptors and the effects on their transactivational properties.* Mol Cell Endocrinol, 2000. **167**(1-2): p. 139-50.
100. Peters, A.A., et al., *Androgen receptor inhibits estrogen receptor-alpha activity and is prognostic in breast cancer.* Cancer Res, 2009. **69**(15): p. 6131-40.
101. Sanchez-Criado, J.E., et al., *Estrogen receptor (ESR) 2 partially offsets the absence of ESR1 in gonadotropes of pituitary-specific Esr1 knockout female mice.* Reproduction, 2012. **143**(4): p. 549-58.

102. Rosenfeld, C.S., et al., *Transcription and translation of estrogen receptor-beta in the male reproductive tract of estrogen receptor-alpha knock-out and wild-type mice.* Endocrinology, 1998. **139**(6): p. 2982-7.
103. Gould, M.L., P.R. Hurst, and H.D. Nicholson, *The effects of oestrogen receptors alpha and beta on testicular cell number and steroidogenesis in mice.* Reproduction, 2007. **134**(2): p. 271-9.
104. Murray, S.A., et al., *Beyond knockouts: cre resources for conditional mutagenesis.* Mamm Genome, 2012. **23**(9-10): p. 587-99.
105. Monroe, D.G., et al., *Estrogen receptor isoform-specific regulation of endogenous gene expression in human osteoblastic cell lines expressing either ERalpha or ERbeta.* J Cell Biochem, 2003. **90**(2): p. 315-26.
106. Reese, J.M., et al., *ERbeta-mediated induction of cystatins results in suppression of TGFbeta signaling and inhibition of triple-negative breast cancer metastasis.* Proc Natl Acad Sci U S A, 2018. **115**(41): p. E9580-E9589.
107. Nelson, J.D., et al., *Fast chromatin immunoprecipitation assay.* Nucleic Acids Res, 2006. **34**(1): p. e2.
108. Langmead, B. and S.L. Salzberg, *Fast gapped-read alignment with Bowtie 2.* Nat Methods, 2012. **9**(4): p. 357-9.
109. Zhang, Y., et al., *Model-based analysis of ChIP-Seq (MACS).* Genome Biol, 2008. **9**(9): p. R137.
110. Dobin, A., et al., *STAR: ultrafast universal RNA-seq aligner.* Bioinformatics, 2013. **29**(1): p. 15-21.
111. Love, M.I., W. Huber, and S. Anders, *Moderated estimation of fold change and dispersion for RNA-seq data with DESeq2.* Genome Biol, 2014. **15**(12): p. 550.
112. Lu, M., et al., *Insulin regulates liver metabolism in vivo in the absence of hepatic Akt and Foxo1.* Nat Med, 2012. **18**(3): p. 388-95.
113. Einstein, F.H., et al., *Aging per se increases the susceptibility to free fatty acid-induced insulin resistance.* J Gerontol A Biol Sci Med Sci, 2010. **65**(8): p. 800-8.
114. Huffman, D.M., et al., *Central insulin-like growth factor-1 (IGF-1) restores whole-body insulin action in a model of age-related insulin resistance and IGF-1 decline.* Aging Cell, 2016. **15**(1): p. 181-6.
115. Ayala, J.E., et al., *Standard operating procedures for describing and performing metabolic tests of glucose homeostasis in mice.* Dis Model Mech, 2010. **3**(9-10): p. 525-34.
116. Huffman, D.M., et al., *Evaluating Health Span in Preclinical Models of Aging and Disease: Guidelines, Challenges, and Opportunities for Geroscience.* J Gerontol A Biol Sci Med Sci, 2016. **71**(11): p. 1395-1406.
117. Leonard, A.K., et al., *Methods for the visualization and analysis of extracellular matrix protein structure and degradation.* Methods Cell Biol, 2018. **143**: p. 79-95.
118. Mehlem, A., et al., *Imaging of neutral lipids by oil red O for analyzing the metabolic status in health and disease.* Nat Protoc, 2013. **8**(6): p. 1149-54.
119. Folch, J., M. Lees, and G.H. Sloane Stanley, *A simple method for the isolation and purification of total lipides from animal tissues.* The Journal of biological chemistry, 1957. **226**(1): p. 497-509.
120. Stout, M.B., L.F. Liu, and M.A. Belury, *Hepatic steatosis by dietary-conjugated linoleic acid is accompanied by accumulation of diacylglycerol and increased membrane-associated protein kinase C epsilon in mice.* Mol Nutr Food Res, 2011. **55**(7): p. 1010-7.
121. Agbaga, M.P., et al., *Differential composition of DHA and very-long-chain PUFAs in rod and cone photoreceptors.* J Lipid Res, 2018. **59**(9): p. 1586-1596.
122. Yu, M., et al., *ELOVL4 protein preferentially elongates 20:5n3 to very long chain PUFAs over 20:4n6 and 22:6n3.* J Lipid Res, 2012. **53**(3): p. 494-504.
123. Quehenberger, O., et al., *Lipidomics reveals a remarkable diversity of lipids in human plasma.* J Lipid Res, 2010. **51**(11): p. 3299-305.
124. Livak, K.J. and T.D. Schmittgen, *Analysis of relative gene expression data using real-time quantitative PCR and the 2(-Delta Delta C(T)) Method.* Methods, 2001. **25**(4): p. 402-8.

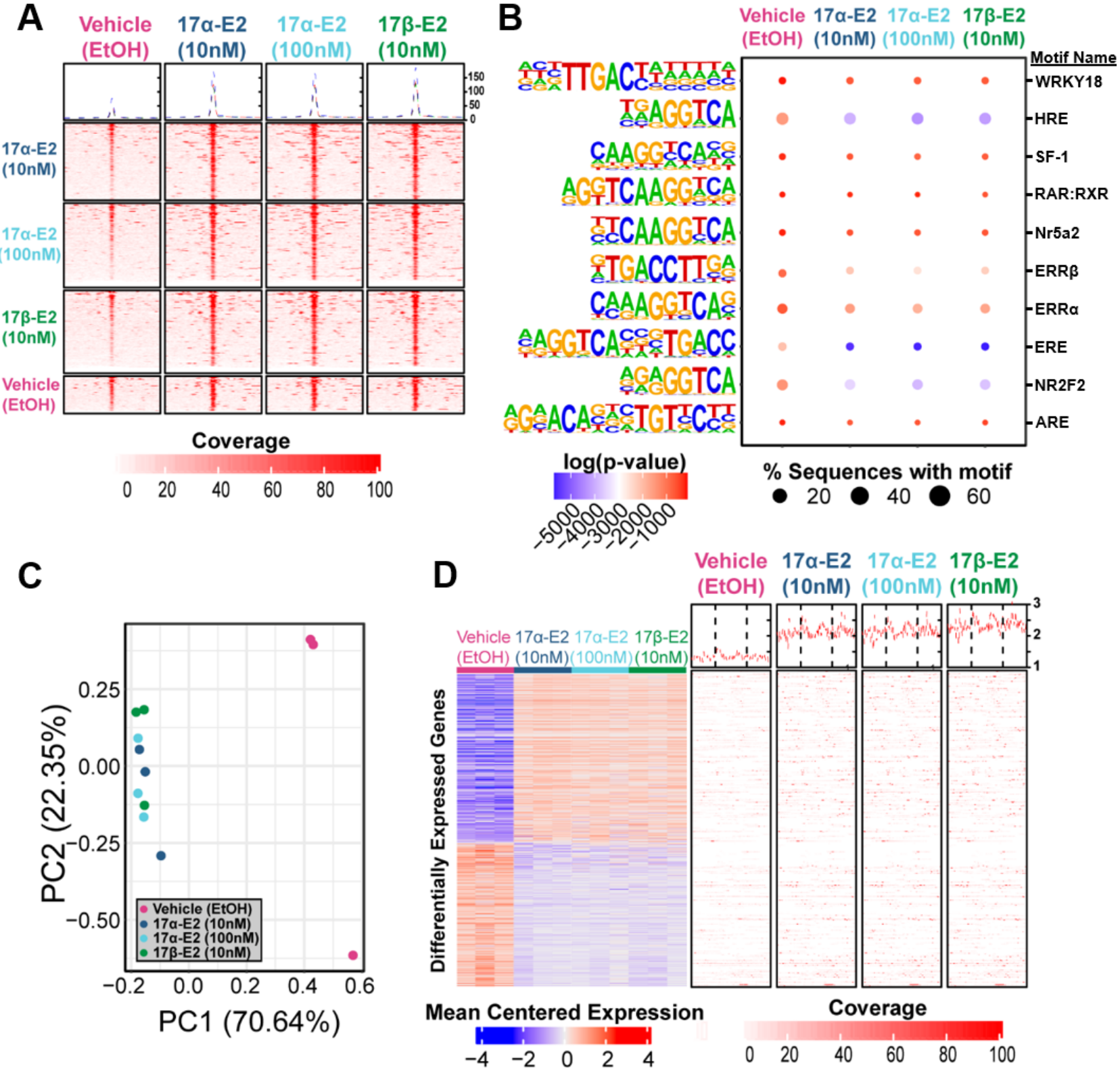

Figure 1

Figure 1. 17α-E2 and 17β-E2 elicit similar transcriptional profiles through ERα. (A) Heatmap representing normalized genome-wide DNA binding by ERα via ChIP sequencing analyses centered according to peak summits for each treatment group, (B) Motif enrichment analysis showing top 10 enriched sequence motifs enriched across treatment groups, (C) PCA plot of transcriptional profiles by RNA sequencing analyses, and (D) Heatmap representing differentially-expressed genes by RNA sequencing analyses (left) and ERα binding patterns within the gene body ±5 kb flanking regions of these genes identified by ChIP sequencing (right). These studies utilized U2OS-ERα cells treated with low dose (10nM) 17α-E2, high dose (100nM) 17α-E2, 17β-E2 (10nM), or vehicle (EtOH). n=3/group.

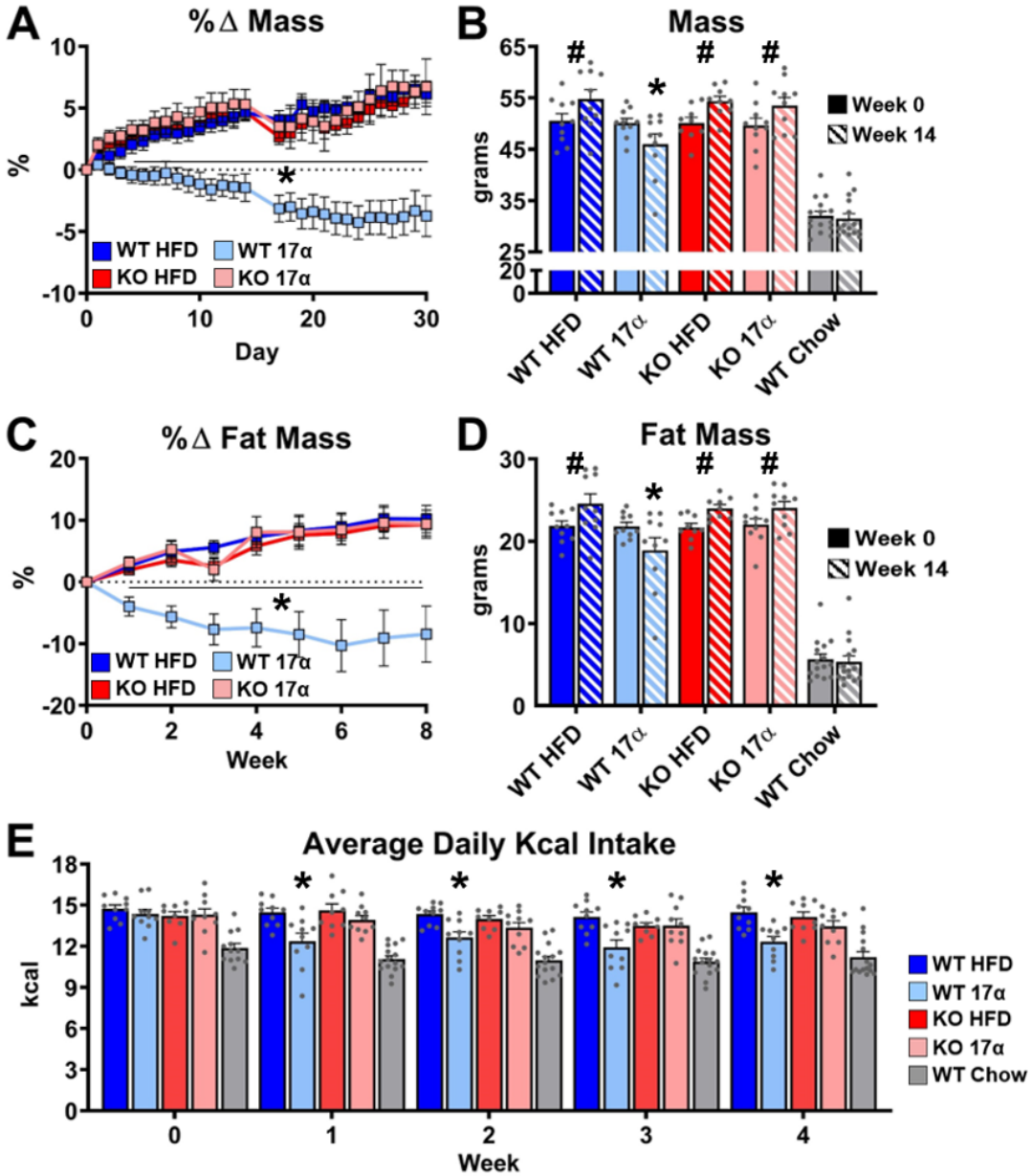

Figure 2. Functional ERα is required for 17α-E2 to reduce mass, adiposity, and calorie intake in male mice. (A) Daily percent change in mass, (B) Mass at baseline (week 0; solid) and week 14 (striped), (C) Weekly percent change in fat mass, (D) Fat mass at baseline (week 0; solid) and week 14 (striped), and (E) Average daily calorie intake per week in WT and ERα KO mice provided 45% HFD (TestDiet 58V8) ± 17α-E2 (14.4 mg/kg). Age-matched, WT, chow-fed (TestDiet 58YP) controls (grey bars) were also evaluated and the corresponding data is shown for visual comparison purposes. All data are presented as mean ± SEM and were analyzed by 2-way repeated measures ANOVA with the WT Chow group being excluded from statistical comparisons. * # $p<0.05$. * indicates significance between WT HFD and WT 17α within the same timepoint. # indicates significance between week 0 and week 14 within the same treatment group. n = 10 (WT HFD), 10 (WT 17α), 10 (KO HFD), 10 (KO 17α), 12-15 (WT Chow).

Figure 3

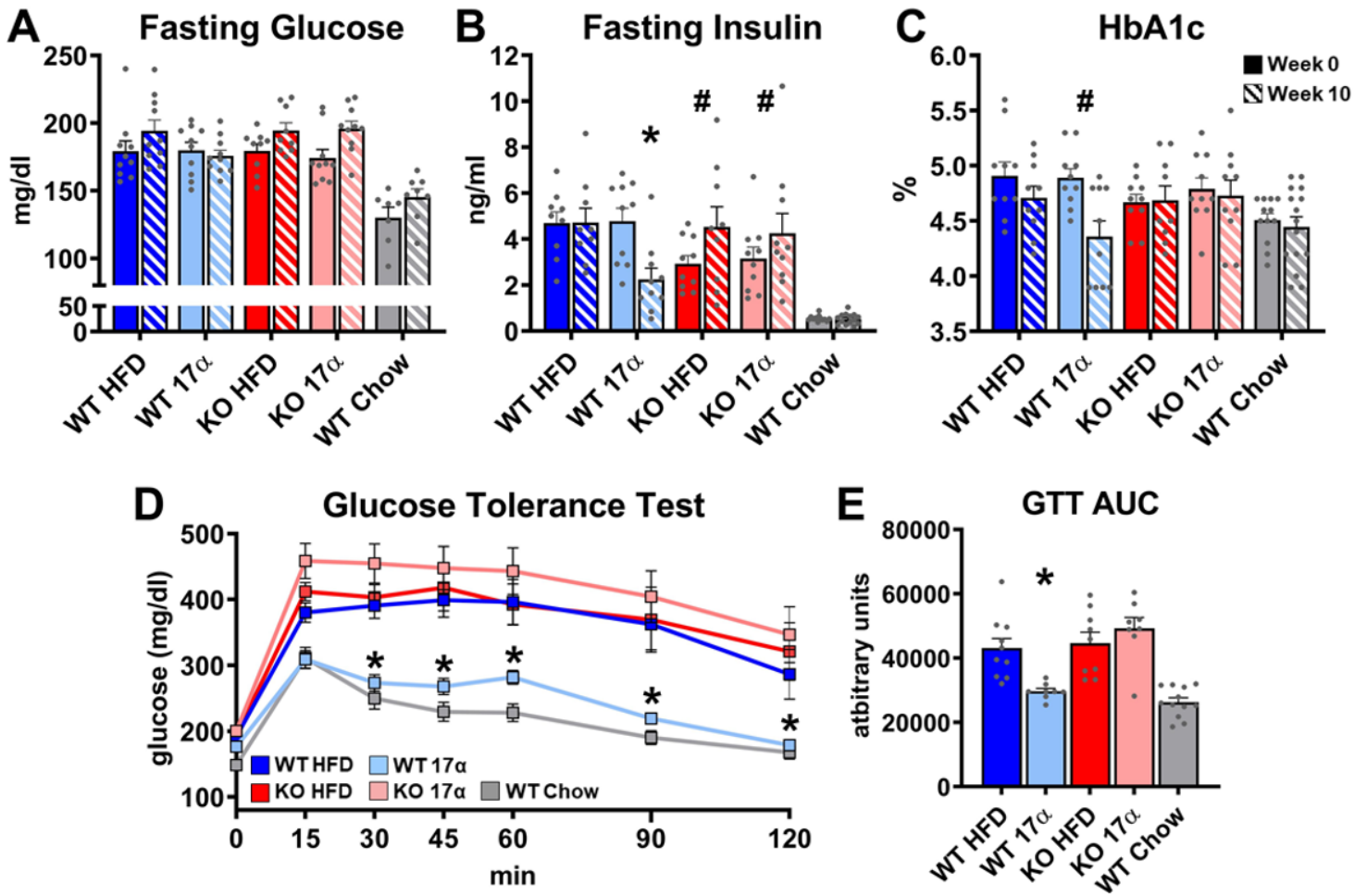

Figure 3. 17α-E2 reverses obesity-related metabolic dysfunction in male WT, but not ERα KO, mice. (A) Fasting glucose, (B) Fasting insulin, and (C) glycosylated hemoglobin (HbA1c) at baseline (week 0; solid) and week 14 (striped) in WT and ERα KO mice provided 45% HFD (TestDiet 58V8) ± 17α-E2 (14.4 mg/kg). (D) Glucose tolerance testing (GTT; 1mg/kg) and (E) GTT AUC during week 10 of the study. Age-matched, WT, chow-fed (TestDiet 58YP) controls (grey bars) were also evaluated and the corresponding data is shown for visual comparison purposes. All data are presented as mean ± SEM and were analyzed by 2-way repeated measures ANOVA or 2-way ANOVA with the WT Chow group being excluded from statistical comparisons. * # $p<0.05$. * indicates significance between WT HFD and WT 17α within the same timepoint. # indicates significance between week 0 and week 10 within the same treatment group. n = 9-10 (WT HFD), 8-10 (WT 17α), 9-10 (KO HFD), 8-10 (KO 17α), 12-15 (WT Chow).

Figure 4

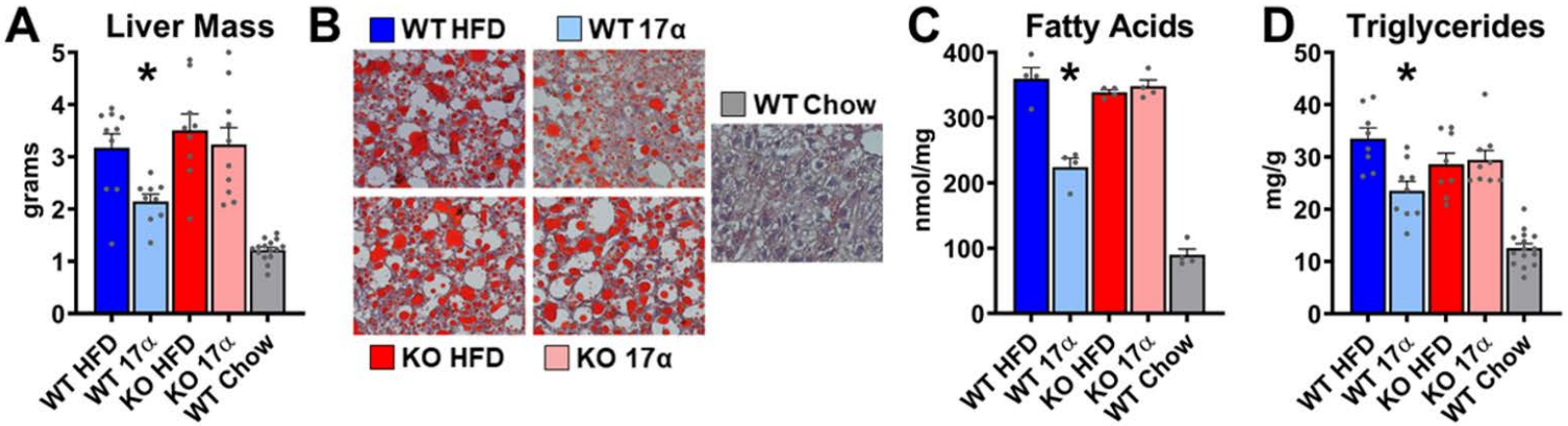

Figure 4. 17α-E2 reverses obesity-related hepatic steatosis in an ERα-dependent manner in male mice. (A) Liver mass, (B) Representative liver oil-red-O staining, (C) Liver fatty acids, and (D) Liver triglycerides in WT and ERα KO mice provided 45% HFD (TestDiet 58V8) ± 17α-E2 (14.4 mg/kg) for 14 weeks. Age-matched, WT, chow-fed (TestDiet 58YP) controls (grey bars) were also evaluated and the corresponding data is shown for visual comparison purposes. All data are presented as mean ± SEM and were analyzed by 2-way ANOVA with the WT Chow group being excluded from statistical comparisons. * $p<0.05$. n = 4-10 (WT HFD), 4-9 (WT 17α), 4-9 (KO HFD), 4-10 (KO 17α), 4-15 (WT Chow).

Figure 5

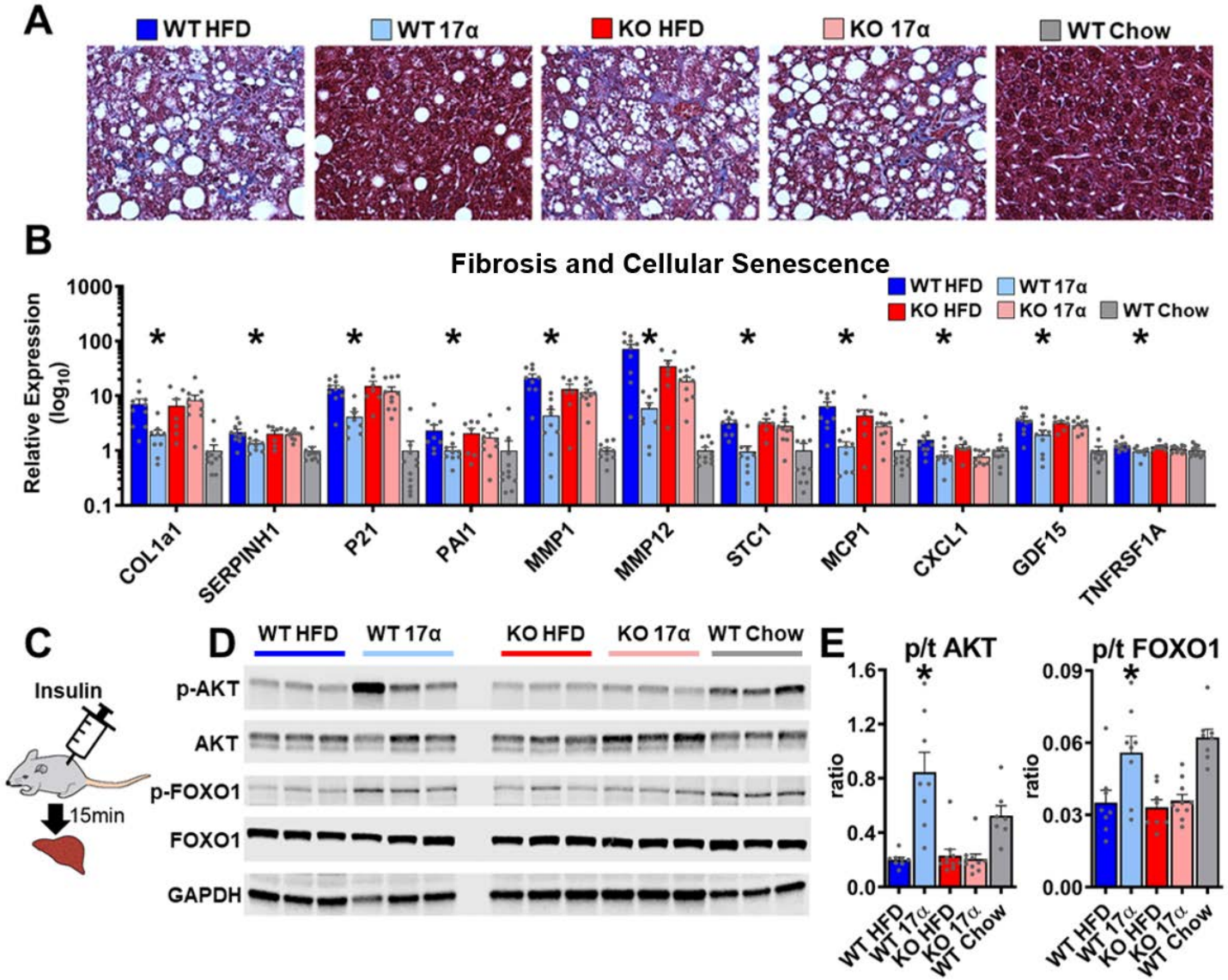

Figure 5. 17α-E2 reverses obesity-related liver fibrosis, senescence, and insulin resistance in an ERα-dependent manner in male mice. (A) Representative liver Masson's trichrome staining for collagen and (B) Liver transcriptional markers of fibrosis, senescence, and SASP in WT and ERα KO mice provided 45% HFD (TestDiet 58V8) ± 17α-E2 (14.4 mg/kg) for 14 weeks. (C) Schematic of *in vivo* insulin stimulation (2mU/g) in fasting mice, (D) Representative liver immunoblots, and (E) Quantification of phospho/total (p/t) AKT (pS473) and FOXO1 (pS256) in WT and ERα KO mice provided 60% HFD (TestDiet 58Y1) ± 17α-E2 (14.4 mg/kg) for 12 weeks. Age-matched, WT, chow-fed (TestDiet 58YP) controls (grey bars) were also evaluated in both animal studies and the corresponding data is shown for visual comparison purposes. All data are presented as mean ± SEM and were analyzed by 2-way ANOVA with the WT Chow group being excluded from statistical comparisons. * $p<0.05$. n = 8-10 (WT HFD), 8-9 (WT 17α), 7-10 (KO HFD), 10 (KO 17α), 7-11 (WT Chow).

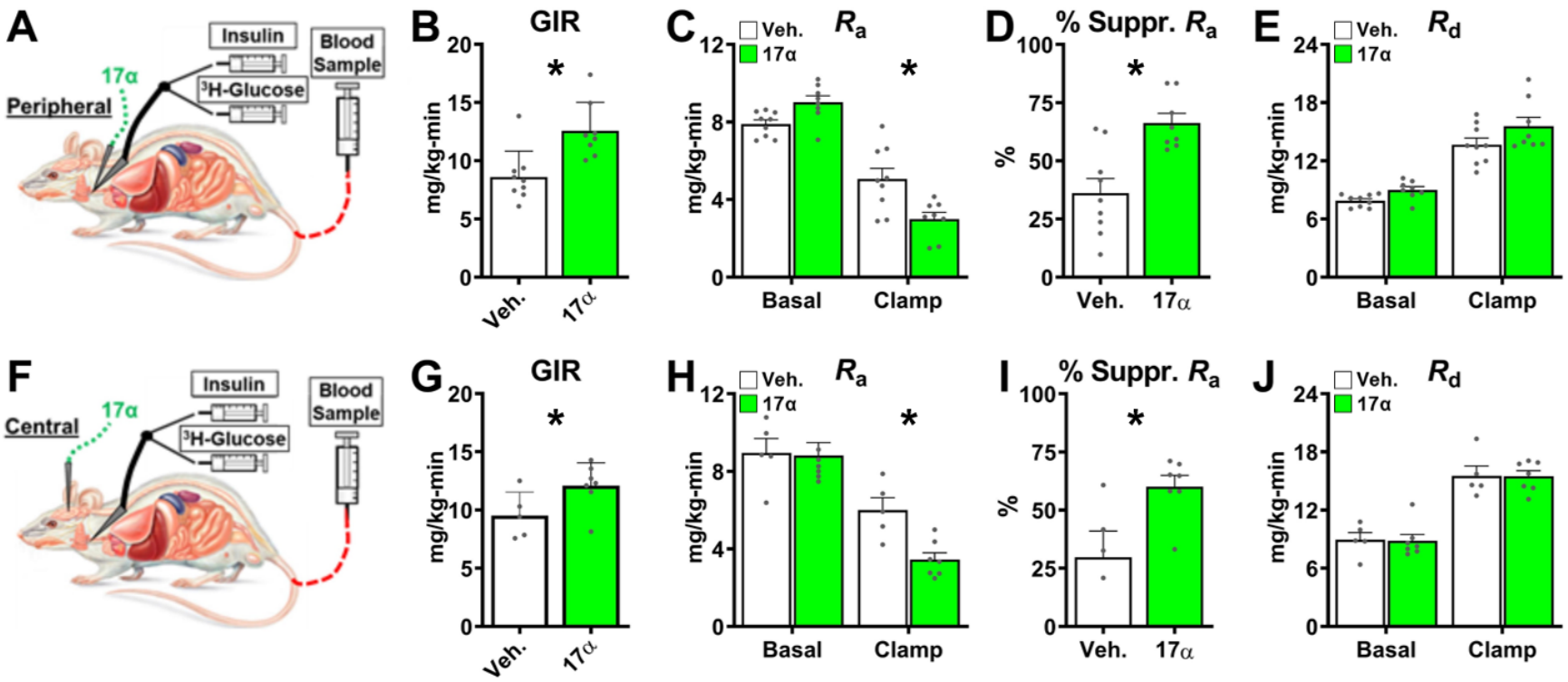

Figure 6. Acute delivery of 17α-E2 improves hepatic insulin sensitivity. (A) Schematic of peripheral 17α-E2 infusions (or vehicle) during hyperinsulinemic-euglycemic clamps, (B) Glucose infusion rates (GIR), (C) Rate of glucose appearance (R_a; hepatic glucose production), (D) % suppression of hepatic glucose production, and (D) Rate of glucose disappearance (R_d; peripheral glucose disposal) in 6-month old, male, FBN-F1 hybrid rats. (F) Schematic of ICV (central) 17α-E2 infusions (or vehicle) during hyperinsulinemic-euglycemic clamps, (G) GIR, (H) R_a, (I) % suppression glucose production, and (J) R_d in 6-month old, male, FBN-F1 hybrid rats. All data are presented as mean ± SEM and were analyzed by Student's t-test. * $p<0.05$. n = 5-9 (CON), 7-8 (17α).

Supplementary Figure 1

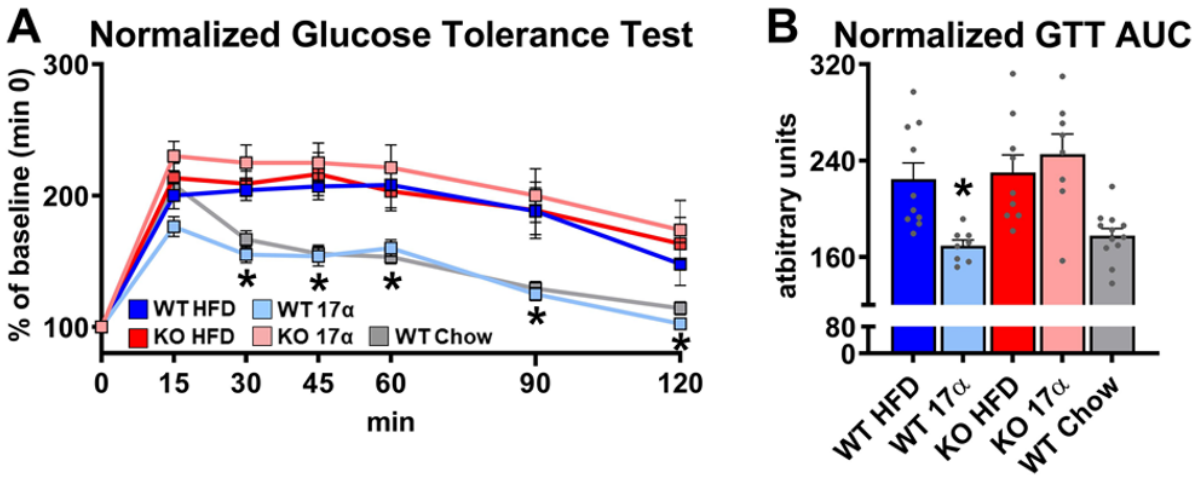

Supplementary Figure 1. 17α-E2 reverses obesity-related metabolic dysfunction in male WT, but not ERα KO, mice. (A) Glucose tolerance testing (GTT; 1mg/kg), normalized to baseline (min 0), and (B) Normalized GTT AUC in WT and ERα KO mice provided 45% HFD (TestDiet 58V8) ± 17α-E2 (14.4 mg/kg) for 10 weeks. Age-matched, WT, chow-fed (TestDiet 58YP) controls (grey bars) were also evaluated and the corresponding data is shown for visual comparison purposes. All data are presented as mean ± SEM and were analyzed by 2-way repeated measures ANOVA or 2-way ANOVA with the WT Chow group being excluded from statistical comparisons. * $p<0.05$. n = 10 (WT HFD), 8 (WT 17α), 9 (KO HFD), 8 (KO 17α), 12 (WT Chow).

Supplementary Figure 2

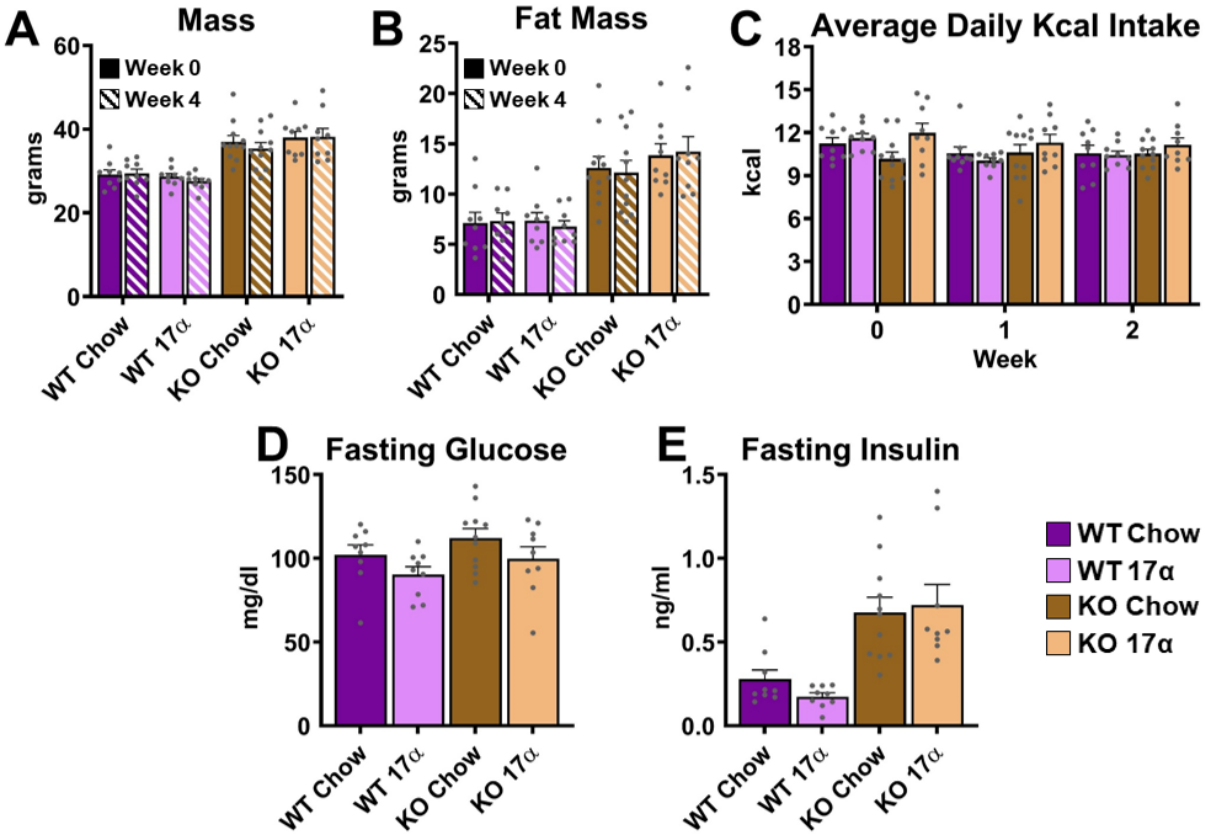

Supplementary Figure 2. 17α-E2 fails to alter metabolic parameters in WT or ERα KO female mice. (A) Mass at baseline (week 0; solid) and week 4 (striped), (B) Fat mass at baseline (week 0; solid) and week 4 (striped), (C) Average daily calorie intake per week, (D) Fasting glucose during week 4, and (E) Fasting insulin during week 4 in WT and ERα KO female mice provided chow (TestDiet 58YP) ± 17α-E2 (14.4 mg/kg). All data are presented as mean ± SEM and were analyzed by 2-way repeated measures ANOVA or 2-way ANOVA. $p<0.05$. n = 9 (WT Chow), 9 (WT 17α), 11 (KO Chow), 9 (KO 17α).

Supplementary Figure 3

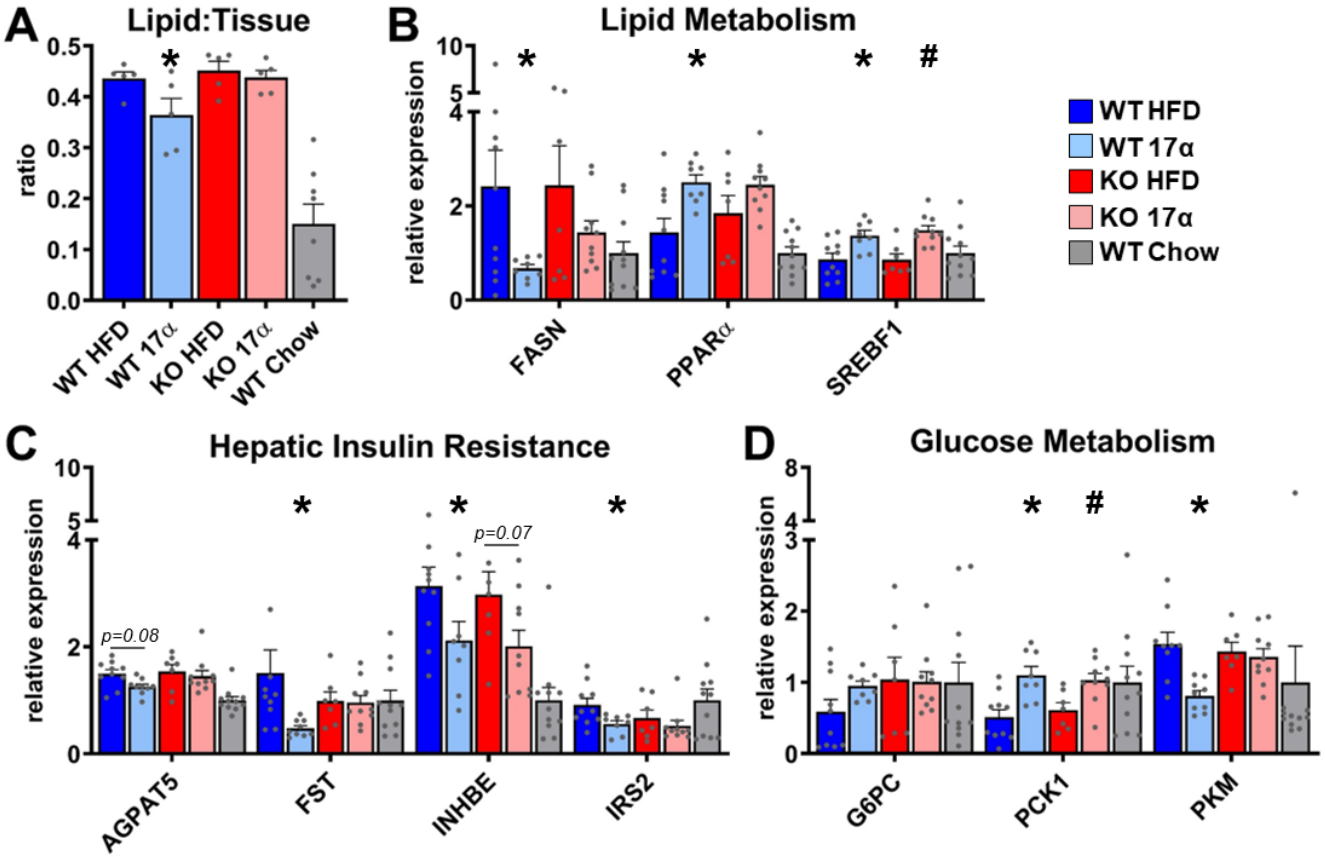

Supplementary Figure 3. 17α-E2 alters markers of lipid and glucose homeostasis predominantly through in male mice. (A) Quantification of oil-red-O lipid staining in liver sections from WT and ERα KO mice provided 45% HFD (TestDiet 58V8) ± 17α-E2 (14.4 mg/kg) for 14 weeks. Hepatic gene expression related to (B) Lipid metabolism, (C) Hepatic insulin resistance, and (D) Glucose homeostasis from WT and ERα KO mice provided 45% HFD (TestDiet 58V8) ± 17α-E2 (14.4 mg/kg) for 14 weeks. Age-matched, WT, chow-fed (TestDiet 58YP) controls (grey bars) were also evaluated and the corresponding data is shown for visual comparison purposes. All data are presented as mean ± SEM and were analyzed by 2-way ANOVA with the WT Chow group being excluded from statistical comparisons. * # $p<0.05$. * indicates significance between WT HFD and WT 17α. # indicates significance between KO HFD and KO 17α. n = 5-10 (WT HFD), 5-9 (WT 17α), 5-7 (KO HFD), 5-10 (KO 17α), 8-11 (WT Chow).

Supplementary Figure 4

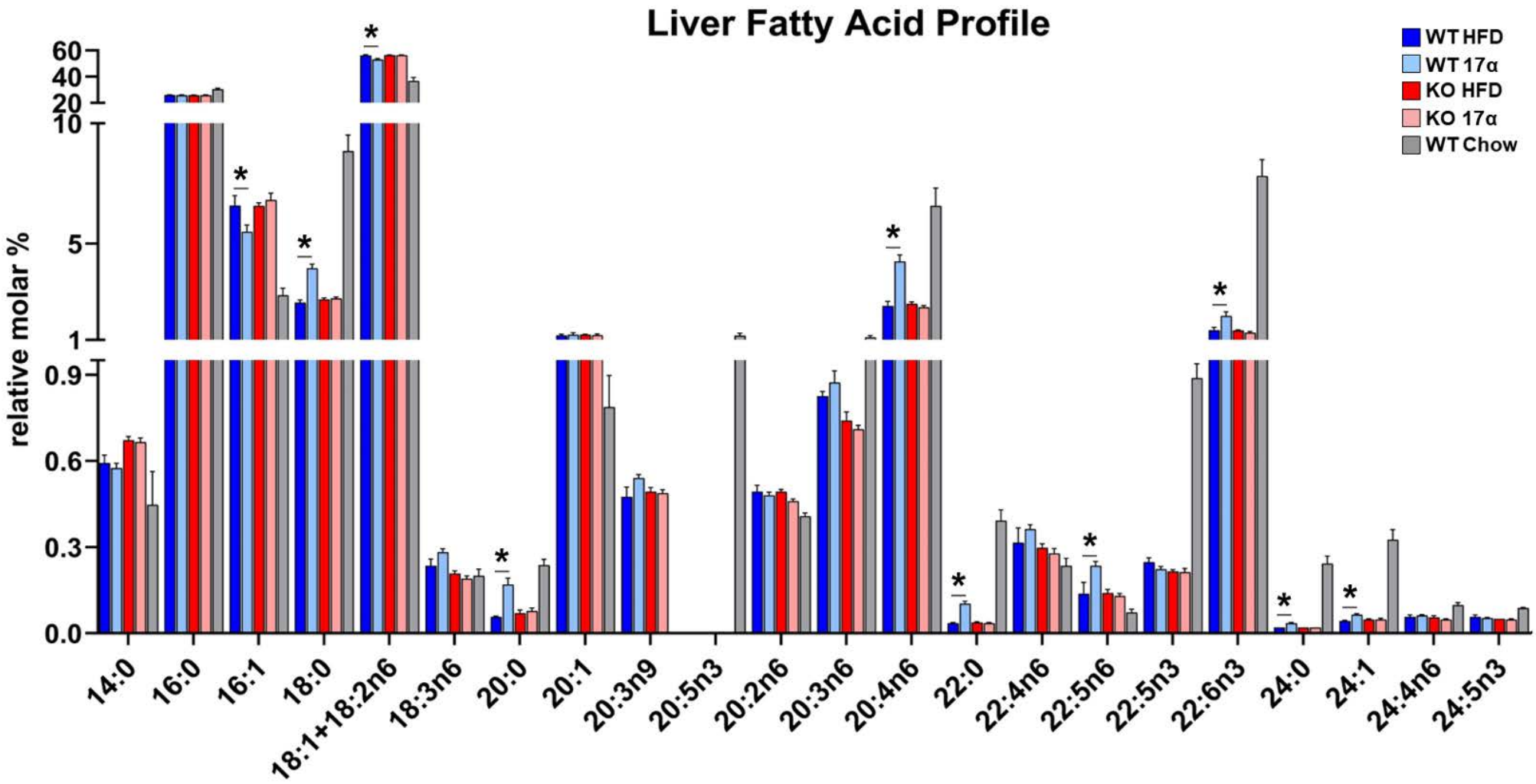

Supplementary Figure 4. 17α-E2 alters the hepatic fatty acid profile in male WT, but not ERα KO, mice. Relative molar % of fatty acids in the liver from WT and ERα KO mice provided 45% HFD (TestDiet 58V8) ± 17α-E2 (14.4 mg/kg) for 14 weeks. Age-matched, WT, chow-fed (TestDiet 58YP) controls (grey bars) were also evaluated and the corresponding data is shown for visual comparison purposes. All data are presented as mean ± SEM and were analyzed by 2-way ANOVA with the WT Chow group being excluded from statistical comparisons. * $p<0.05$. n = 4.

Supplementary Table 1. Circulating eicosanoid levels (pmol/ml)

Systematic Name	Common Name	WT HFD	WT 17α	Chow	*p-value*
12-hydroxy-5Z,8Z,10E,14Z-eicosatetraenoic acid	**12-HETE**	**104.7** ± 28.77	**124.6** ± 30.29	**47.7** ± 10.28	0.642
12-oxo-5Z,8Z,10E,14Z-eicosatetraenoic acid	**12-OxoETE**	**183.5** ± 68.65	**97.9** ± 49.40	**11.5** ± 5.18	0.332
(+/-)-14-hydroxy-4Z,7Z,10Z,12E,16Z,19Z-docosahexaenoic acid	**14-HDoHE**	**29.2** ± 9.93	**26.1** ± 7.76	**132.4** ± 56.52	0.813
13-hydroxy-9Z,11E-octadecadienoic acid	**13-HODE**	**18.7** ± 2.07	**23.4** ± 2.25	**96.6** ± 10.60	0.146
7,17-dihydroxy-(8Z,10,13,15E,19Z)-docosapentaenoic acid	**7,17-dHDPA**	**14.77** ± 2.19	**16.45** ± 1.98	**20.88** ± 5.24	0.580
(+/-)-19,20-dihydroxy-4Z,7Z,10Z,13Z,16Z-docosapentaenoic acid	**19,20-DiHDPA**	**13.49** ± 1.84	**14.27** ± 1.89	**20.59** ± 5.66	0.772
9-hydroxy-10E,12Z-octadecadienoic acid	**9-HODE**	**12.06** ± 0.94	**13.11** ± 1.22	**161.47** ± 26.72	0.507
12,13-dihydroxy-9Z-octadecenoate	**12,13-diHOME**	**9.23** ± 1.33	**10.06** ± 1.14	**70.04** ± 10.25	0.644
12S-hydroxy-5Z,8E,10E-heptadecatrienoic acid	**12-HHTrE**	**3.32** ± 0.29	**9.57** ± 3.78	**7.12** ± 1.42	***0.075***
5S-hydroxy-6E,8Z,11Z,14Z-eicosatetraenoic acid	**5-HETE**	**7.84** ± 0.47	**9.31** ± 1.25	**5.49** ± 0.28	0.291
tetranor 13,14-dihydro-15-keto prostaglandin E2	**Tetranor-PGEM**	**8.95** ± 1.11	**9.14** ± 1.45	**8.68** ± 0.57	0.920
(+/-)-12(13)-epoxy-9Z-octadecenoic acid	**12(13)-EpOME**	**5.31** ± 0.39	**8.07** ± 1.62	**16.42** ± 0.96	0.123
(+/-)-19(20)-epoxy-4Z,7Z,10Z,13Z,16Z-docosapentaenoic acid	**19(20)-EpDPE**	**6.55** ± 0.44	**7.83** ± 0.45	**20.12** ± 2.76	***0.065***
13S-hydroxy-6Z,9Z,11E-octadecatrienoic acid	**13-HOTrE**	**5.77** ± 0.55	**7.76** ± 1.33	**13.14** ± 1.85	0.193
14,15-dihydroxy-5Z,8Z,11Z-eicosatrienoic acid	**14,15-diHETrE**	**4.75** ± 0.61	**6.02** ± 0.85	**2.29** ± 0.48	0.250
(+/-)-12-hydroxy-5Z,8Z,10E,14Z,17Z-eicosapentaenoic acid	**12-HEPE**	**9.64** ± 3.78	**6.00** ± 1.96	**126.98** ± 56.06	0.410
13-keto-9Z,11E-octadecadienoic acid	**13-OxoODE**	**5.59** ± 0.69	**4.22** ± 0.88	**6.17** ± 0.81	0.258
11,12-epoxy-5Z,8Z,14Z-eicosatrienoic acid	**11(12)-EET**	**2.61** ± 0.15	**3.90** ± 0.74	**2.64** ± 0.33	0.113
8S-hydroxy-5Z,9E,11Z,14Z-eicosatetraenoic acid	**8-HETE**	**3.77** ± 0.37	**3.67** ± 0.65	**4.78** ± 2.21	0.900
9,10-dihydroxy-12Z-octadecenoic acid	**9,10-diHOME**	**4.19** ± 0.65	**3.43** ± 0.36	**23.67** ± 2.89	0.326
8,9-epoxy-5Z,11Z,14Z-eicosatrienoic acid	**8(9)-EET**	**1.86** ± 0.31	**3.31** ± 0.75	**1.70** ± 0.24	***0.097***
5,6-epoxy-8Z,11Z,14Z-eicosatrienoic acid	**5(6)-EET**	**1.81** ± 0.21	**3.19** ± 0.92	**2.05** ± 0.29	0.168
8,9-dihydroxy-5Z,11Z,14Z-eicosatrienoic acid	**8,9-diHETrE**	**4.08** ± 0.53	**3.17** ± 0.36	**1.65** ± 0.16	0.179
11,12-dihydroxy-5Z,8Z,14Z-eicosatrienoic acid	**11,12-diHETrE**	**3.11** ± 0.43	**2.93** ± 0.42	**1.64** ± 0.34	0.762
9,10-epoxy-12Z-octadecenoic acid	**9(10)-EpOME**	**1.42** ± 0.12	**2.83** ± 0.86	**6.63** ± 0.94	0.129

17α-E2 mildly alters the circulating eicosanoid profile in obese middle-aged male mice. WT mice were provided 45% HFD (TestDiet 58V8) ± 17α-E2 (14.4 mg/kg) for 14 weeks. Age-matched, WT, chow-fed (TestDiet 58YP) controls were also evaluated and the corresponding data is shown for comparison purposes. All data are presented as mean ± SEM and were analyzed by Student's t-test with the WT Chow group being excluded from statistical comparisons. n = 5-7.

Supplementary Table 1. Circulating eicosanoid levels (pmol/ml)

Systematic Name	Common Name	WT HFD	WT 17α	Chow	*p-value*
15S-hydroxy-5Z,8Z,11Z,13E-eicosatetraenoic acid	**15-HETE**	**1.29** ± 0.15	**2.24** ± 0.51	**3.17** ± 1.96	***0.098***
5,6-dihydroxy-8Z,11Z,14Z-eicosatrienoic acid	**5,6-DiHETrE**	**2.76** ± 0.40	**2.17** ± 0.24	**1.09** ± 0.14	0.228
8S-hydroxy-9E,11Z,14Z-eicosatrienoic acid	**8-HETrE**	**0.58** ± 0.13	**0.56** ± 0.08	**0.64** ± 0.13	0.872
(+/-)-16-hydroxy-4Z,7Z,10Z,13Z,17E,19Z-docosahexaenoic acid	**16-HDoHE**	**0.46** ± 0.06	**0.61** ± 0.13	**2.52** ± 0.28	0.314
17-hydroxy-5Z,8Z,11Z,14Z-eicosatetraenoic acid	**17-HETE**	**0.53** ± 0.06	**0.61** ± 0.06	**0.32** ± 0.03	0.337
9S-hydroxy-10E,12Z,15Z-octadecatrienoic acid	**9-HOTrE**	**0.72** ± 0.10	**0.67** ± 0.11	**15.58** ± 3.38	0.728
(+/-)-16(17)-epoxy-4Z,7Z,10Z,13Z,19Z-docosapentaenoic acid	**16(17)-EpDPE**	**0.64** ± 0.10	**0.70** ± 0.13	**2.34** ± 0.30	0.754
16-hydroxy-5Z,8Z,11Z,14Z-eicosatetraenoic acid	**16-HETE**	**0.63** ± 0.10	**0.72** ± 0.18	**0.52** ± 0.15	0.690
5S,15S-dihydroxy-6E,8Z,11Z,13E-eicosatetraenoic acid	**5,15-diHETE**	**0.69** ± 0.08	**0.76** ± 0.07	**0.74** ± 0.16	0.497
(+/-)-11-hydroxy-4Z,7Z,9E,13Z,16Z,19Z-docosahexaenoic acid	**11-HDoHE**	**0.98** ± 0.34	**0.82** ± 0.18	**2.94** ± 0.26	0.739
15S-hydroxy-8Z,11Z,13E-eicosatrienoic acid	**15-HETrE**	**0.80** ± 0.13	**0.87** ± 0.13	**1.03** ± 0.40	0.725
(+/-)-10-hydroxy-4Z,7Z,11E,13Z,16Z,19Z-docosahexaenoic acid	**10-HDoHE**	**0.96** ± 0.25	**0.93** ± 0.24	**5.96** ± 2.09	0.917
(+/-)-7-hydroxy-4Z,8E,10Z,13Z,16Z,19Z-docosahexaenoic acid	**7-HDoHE**	**1.16** ± 0.22	**0.93** ± 0.11	**2.98** ± 0.24	0.331
8R-hydroxy-4Z,6E,10Z-hexadecatrienoic acid	**Tetranor 12-HETE**	**1.02** ± 0.15	**0.96** ± 0.17	**0.91** ± 0.19	0.796
11S-hydroxy-5Z,8Z,11E,14Z-eicosatetraenoic acid	**11-HETE**	**0.70** ± 0.07	**1.13** ± 0.17	**0.53** ± 0.10	***0.039***
9S,11,15S-trihydroxy-thromboxa-5Z,13E-dien-1-oic acid	**TXB2**	**0.60** ± 0.08	**1.21** ± 0.54	**17.92** ± 17.41	0.249
dihydro-ketoprostaglandin D(2)	**dhk-PGD2**	**1.11** ± 0.09	**1.26** ± 0.07	**1.15** ± 0.07	0.192
14S,15R-epoxy-5Z,8Z,11Z-eicosatrienoic acid	**14(15)-EET**	**0.93** ± 0.13	**1.40** ± 0.23	**1.09** ± 0.21	***0.097***
(+/-)-4-hydroxy-5E,7Z,10Z,13Z,16Z,19Z-docosahexaenoic acid	**4-HDoHE**	**1.63** ± 0.26	**1.59** ± 0.31	**5.72** ± 0.34	0.923
(+/-)-8-hydroxy-4Z,6E,10Z,13Z,16Z,19Z-docosahexaenoic acid	**8-HDoHE**	**1.78** ± 0.19	**1.69** ± 0.22	**8.40** ± 1.02	0.782
10E,12Z-9-oxoode	**9-OxoODE**	**1.08** ± 0.18	**1.70** ± 0.44	**9.56** ± 1.01	0.220
9-hydroxy-5Z,7E,11Z,14Z-eicosatetraenoic acid	**9-HETE**	**1.80** ± 0.39	**1.72** ± 0.25	**1.43** ± 0.05	0.879
20-hydroxy-5Z,8Z,11Z,14Z-eicosatetraenoic acid	**20-HETE**	**2.28** ± 0.28	**1.85** ± 0.15	**2.10** ± 0.28	0.223
20-carboxy arachidonic acid	**20-COOHAA**	**2.17** ± 0.38	**1.87** ± 0.20	**1.35** ± 0.33	0.505
18-hydroxy-5Z,8Z,11Z,14Z-eicosatetraenoic acid	**18-HETE**	**1.97** ± 0.09	**1.91** ± 0.14	**1.71** ± 0.22	0.729

17α-E2 mildly alters the circulating eicosanoid profile in obese middle-aged male mice. WT mice were provided 45% HFD (TestDiet 58V8) ± 17α-E2 (14.4 mg/kg) for 14 weeks. Age-matched, WT, chow-fed (TestDiet 58YP) controls were also evaluated and the corresponding data is shown for comparison purposes. All data are presented as mean ± SEM and were analyzed by Student's t-test with the WT Chow group being excluded from statistical comparisons. n = 5-7.